https://doi.org/10.5194/egusphere-2026-352
Preprint. Discussion started: 13 February 2026

Improved isoprene emission estimates over the Finnish boreal forest using the MEGANv3.2 model

Manuel Bettineschi[1,*], Arineh Cholakian[2], Victoria Sinclair[1], Katerina Sindelarova[3], Arnaud P. Praplan[4], Steven J. Thomas[1,4], Tuukka Petäjä[1], Federico Bianchi[1], and Giancarlo Ciarelli[1]

[1]Institute for Atmospheric and Earth System Research/Physics, Faculty of Science, University of Helsinki, Helsinki, 00014 Finland
[2]LMD UMR CNRS 8539, ENS, École Polytechnique, Institut Pierre Simon Laplace (IPSL), Route de Saclay, 91128 Palaiseau, France
[3]Department of Atmospheric Physics, Faculty of Mathematics and Physics, Charles University, Prague, V Holešovičkách 2, 18000 Prague 8, Czechia
[4]Atmospheric Composition Research, Finnish Meteorological Institute, Helsinki, 00101, Finland
[*]manuel.bettineschi@helsinki.fi

Abstract. In this study, we present an improved framework for modelling isoprene emissions based on the latest version of the Model of Emissions of Gases and Aerosols from Nature (MEGAN). We use high resolution domain-specific tree cover data, species distributions, and species-specific emission factors, to update isoprene emission factors tailored to the Finnish boreal region. These modifications are implemented in MEGAN and integrated into the WRF-CHIMERE chemistry transport model, enabling a more accurate simulation of biogenic emissions. We perform simulations over three consecutive summer periods for the years 2017, 2018, and 2019. Our results reveal a significant reduction in bias for both isoprene emissions fluxes and concentrations compared to previous versions of MEGAN. We further evaluate a canopy correction model to account for the effects of forest canopy on vertical and horizontal transport of biogenic volatile organic compounds (BVOCs) concentrations. These adjustments additionally reduce the bias in modelled isoprene concentrations. The enhanced representation of isoprene emissions, and the effects of canopy on dispersion processes, both result in overall improvements of SOA formation and transportation, emphasizing the importance of ecosystem-specific modifications in emission models and the inclusion of forest canopy correction in chemical transport models. Our findings highlight the importance of moving beyond broad vegetation categories and incorporating detailed tree species distributions in emission factor calculations, demonstrating that ecosystem-specific adjustments are essential for realistic modelling of biogenic emissions and their impacts on atmospheric chemistry.

1 Introduction

Forests significantly affect the atmospheric composition by emitting and removing a multitude of gases and aerosol particles (Fowler et al., 2009). Among the emissions, biogenic volatile organic compounds (BVOCs) play a crucial role in the atmospheric chemistry and physics, influencing ozone (O_3) production, secondary organic aerosol (SOA) formation, and ultimately the climate (Seinfeld and Pandis, 2016). It is estimated that globally BVOCs emissions account for over 90% of the total volatile organic compounds (VOCs) emissions (Wang et al., 2024b). Around 70% of BVOCs emissions are thought to be produced

https://doi.org/10.5194/egusphere-2026-352
Preprint. Discussion started: 13 February 2026

from tropical trees, while only 3% originate from boreal trees (Guenther et al., 2012). Despite this relatively low contribution arising from boreal forests, previous studies have shown that the biogenic SOA originating from boreal region can affect cloud properties and the climate (Tunved et al., 2006; Paasonen et al., 2013; Yli-Juuti et al., 2021; Petäjä et al., 2022).

BVOCs consist of thousands of different compounds (Peñuelas and Staudt, 2010), among these the most studied and most abundant in the atmosphere are isoprene (C_5H_8) and monoterpenes (e.g., α-pinene, β-pinene, limonene) (Guenther et al., 1995; Laothawornkitkul et al., 2009). Isoprene emissions are estimated to range from 299 to 594 Tg C yr^{-1}, accounting for 41-70% of the global BVOCs emissions, while monoterpenes emissions estimations range from 63 to 184 Tg C yr^{-1}, corresponding to 10-22% of the global BVOCs emissions budget (Arneth et al., 2011; Guenther et al., 2012; Messina et al., 2016; Sindelarova et al., 2014, 2022; Weng et al., 2020; Opacka et al., 2021; Wang et al., 2024a). Isoprene is removed from the atmosphere primarily through its reaction with the OH radical, resulting in a lifetime of about 1.4 hours under typical OH levels (2×10^6 molecule cm^{-3}), and while isoprene can react efficiently also with the NO_3 radical, the absence of night-time isoprene emissions makes this reaction overall less important (Atkinson, 2000; Seinfeld and Pandis, 2016). On the other hand, monoterpenes can react rapidly with all the atmospheric oxidants; OH, O_3, and NO_3, with night-time oxidation also relevant due to non-zero monoterpenes emissions during night (Laffineur et al., 2011; Hakola et al., 2017). The products of the oxidation of these BVOCs are organic gases with a different range of saturation vapor concentration (C^*), these gases can have C^* low enough to transition into the aerosol phase, effectively contributing to new particle formation and aerosol growth (Ehn et al., 2014; Riccobono et al., 2014; Lehtipalo et al., 2018; Bianchi et al., 2019).

Isoprene and monoterpenes contribute to SOA formation with different efficiencies. Previous studies have reported SOA yields for isoprene ranging between 0 and 5% (Edney et al., 2005; Kroll et al., 2006; Ng et al., 2006; Kleindienst et al., 2006; Dommen et al., 2006), showing that, under typical atmospheric conditions, isoprene is not an efficient source of SOA. Monoterpenes SOA yields, in general, present a bigger variability, depending on which monoterpene compound is considered, oxidizing agent, temperature, NOx concentrations, radiation, and relative humidity (Hoffmann et al., 1997; Hoppel et al., 2001; Takekawa et al., 2003; Iinuma et al., 2005; Presto et al., 2005; Zhang et al., 2006; Pathak et al., 2007). Typical SOA yields for monoterpenes oxidation range between 0 and 20%, with yields up to 60% under favorable conditions (Lane et al., 2008). These differences highlight the importance of accurate estimation of BVOCs emissions in order to simulate correctly SOA formation mechanism in global and regional models. For instance, while isoprene contributes to SOA formation with relatively low efficiency, it can also decrease the SOA yield from other BVOCs by scavenging OH radicals and altering the oxidation pathways of monoterpenes (McFiggans et al., 2019), meaning that a bias in emissions of one BVOC can affect SOA yields of other BVOCs.

BVOCs emissions are usually estimated in two ways: a top-down approach based on satellite measurements, which allows BVOCs emissions to be indirectly derived (Harrison et al., 2013), and a bottom-up approach, which is the most widely used and it is the method used in this paper. Bottom-up approaches rely on equations which describe the response of emissions to environmental changes (Guenther et al., 2006, 2012; Messina et al., 2016). The Model of Emission of Gases and Aerosol from Nature (MEGAN) is the most widely used model to calculate BVOCs emissions, and it is an example of a bottom-up model that use empirical equations. MEGAN calculates emissions by multiplying the so-called emission factor (EF) by emissions

https://doi.org/10.5194/egusphere-2026-352
Preprint. Discussion started: 13 February 2026

activity factors, which account for the effects of temperature, radiation, leaf age, soil moisture, CO_2 concentration, and leaf area index (LAI) (Guenther et al., 1995, 2012, 2020). A correct estimation of EFs, defined as the emission under standardized environmental conditions of temperature and solar radiation (Guenther et al., 1995), is particularly important for an accurate representation of emissions in global and regional models. Traditionally, for a given BVOC compound, or class, a single EF is assigned to each plant functional type (PFT). A PFT represents a group of plants sharing the same phylogenetic, phonological and physical characteristics (Prentice et al., 1992), however, in the same PFT coexist many different species with a wide range of EFs (Kesselmeier and Staudt, 1999; Lindfors and Laurila, 2000; Tarvainen et al., 2005; Niinemets et al., 2011; Hakola et al., 2023), making finding a unique EF value to represent the emissions of all the different tree species challenging.

Previous studies utilizing emissions estimated with MEGAN version 2.1 (hereafter MEGANv2.1) showed that in many regions isoprene emissions are greatly overestimated. Ciarelli et al. (2024) performed simulations with WRF-CHIMERE over Europe with a focus on Finland and they showed that at 70% of the stations in Europe isoprene concentrations are overestimated, likely due to an overestimation of emissions due to incorrect EFs. They also showed that the overestimation is particularly high in the boreal region. This is also confirmed by Zhao et al. (2024) where the GEOS-CHEM model was applied over the northern high latitudes, showing a similar isoprene overestimation in boreal forests. Overestimation of isoprene in chemical transport models (CTMs) applications with the MEGANv2.1 model were also reported in the studies focusing on Europe by Jiang et al. (2019) and Cholakian et al. (2022).

The most recent version of MEGAN (hereafter MEGANv3.2) (Guenther et al., 2020) introduced modification in the EFs calculations. The new EFs are not based on PFTs but rather on ecotypes composed by different tree species or tree classes, each with its own EF. However, currently many ecotypes in the standard version of MEGANv3.2 do not contain actual tree species but only a needleleaf/broadleaf divisions, which is ecotype specific, meaning that needleleaf/broadleaf in different ecotypes are considered as different "species" with different species-specific EFs. MEGANv3.2 allows the user to modify the composition of an ecotype and introduce new/different tree species. The utilization of this new feature can potentially result in a better estimations of EFs, when proper input data are used, resulting in lower uncertainties in BVOCs emissions.

While MEGANv2.1 is still the most widely used version, new studies are starting to utilize MEGANv3.2 to create newer BVOCs global emissions inventory or for regional applications. Wang et al. (2024a) applied MEGANv3.2 to estimate global BVOCs emissions from 2001 to 2020. They were able to simulate isoprene and monoterpenes emissions within an order of magnitude at most monitoring stations, although monoterpenes emissions were systematically overestimated. Compared to prior estimates (Arneth et al., 2011; Guenther et al., 2012; Messina et al., 2016; Sindelarova et al., 2014, 2022; Weng et al., 2020; Opacka et al., 2021), their isoprene emissions fall on the lower end of the reported range, while their monoterpenes estimates are the highest. Cholakian et al. (2022) utilized MEGANv3.2 to calculate EFs in the Landes pine forest in southwestern France, accounting for different land-use datasets, including information about the tree species relative presence, which resulted in a better representation of BVOCs concentrations in their simulations compared to using the original EFs from MEGANv2.1.

In this study, we present improved isoprene emissions estimates over the Finnish boreal forest, and a detailed modelling of BVOCs driven aerosol dynamics. Specifically, we: (1) employ MEGANv3.2 to recalculate EFs using high-resolution data on

https://doi.org/10.5194/egusphere-2026-352
Preprint. Discussion started: 13 February 2026

tree species distribution; (2) evaluate the model against measurements of BVOCs emissions and concentrations; (3) evaluate the model against OA concentrations observations; (4) use back-trajectory analysis to give more context to the results and better understand the model's biases. The paper is organized as follows: Section 2 presents the methods including all the details about the simulations; the results are reported in Section 3; Section 4 presents the discussion and recommendations for future BVOCs emissions estimations and BVOCs modelling; finally, Section 5 presents the conclusions of the study.

2 Methods

2.1 WRF-CHIMERE

WRF-CHIMERE v2023r1 (Menut et al., 2024) is a state-of-the-art three-dimensional CTM. It is designed to simulate the emissions, chemical reactions, transport and deposition processes of hundreds of chemical compounds at different vertical and horizontal resolutions. The WRF-CHIMERE model has been extensively utilized in a variety of applications, including inter-comparison exercises (Theobald et al., 2019; Ciarelli et al., 2019; Gao et al., 2024), high-resolution application in: complex terrains (Bessagnet et al., 2020; Vitali et al., 2024; Ciarelli et al., 2025; Bettineschi et al., 2025); urban environments (Falasca and Curci, 2018; Mazzeo et al., 2022); and forest ecosystems (Cholakian et al., 2022; Ciarelli et al., 2024). Additionally, it is a member of the Copernicus Atmosphere Monitoring Services (CAMS) operational ensemble, where it contributes to regional air quality forecasts.

Simulations are conducted for June, July, and August of 2017, 2018, and 2019. The focus on summer months reflects the period when emissions are most concentrated at higher latitudes. In total, three summers, corresponding to nine simulated months, provide a sufficiently representative sample for the analysis. A two-domains configuration with one way nesting is used (see Figure 1), where the parent domain have a resolution of 18km x 18km, while the nested domain covering Finland have a resolution of 6km x 6km. All the simulations are performed "online". The SAPRC-07A chemical mechanism scheme (Carter, 2010) is used for gas-phase chemistry. The partitioning between gas and particles phase of the inorganic aerosols is calculated with the ISORROPIA thermodynamic model (Nenes et al., 1998). OA is represented using the volatility basis set (VBS) framework (Donahue et al., 2006). Oxidation products of VOCs, are divided into four volatility classes with C^* of 1, 10, 100, and 1000 μg m^{-3} (at 300 K), each associated with specific mass yields under low-NOx and high-NOx conditions, as described by Cholakian et al. (2018). The aging processes for anthropogenic secondary organic aerosols (ASOA) and biogenic secondary organic aerosols (BSOA) are modelled with reaction rates of 1×10^{-11} molecule^{-1} cm^3 s^{-1} (Murphy and Pandis, 2009; Cholakian et al., 2018) and 4×10^{-12} molecule^{-1} cm^3 s^{-1} (Bergström et al., 2012; Ciarelli et al., 2024), respectively.

2.1.1 Model input data

Meteorological inputs were generated using version 4.3 of the WRF model (Skamarock et al., 2019). The model was forced with reanalysis data, from the National Centers for Environmental Prediction (NCEP) Climate Forecast System Version 2, at a

https://doi.org/10.5194/egusphere-2026-352
Preprint. Discussion started: 13 February 2026

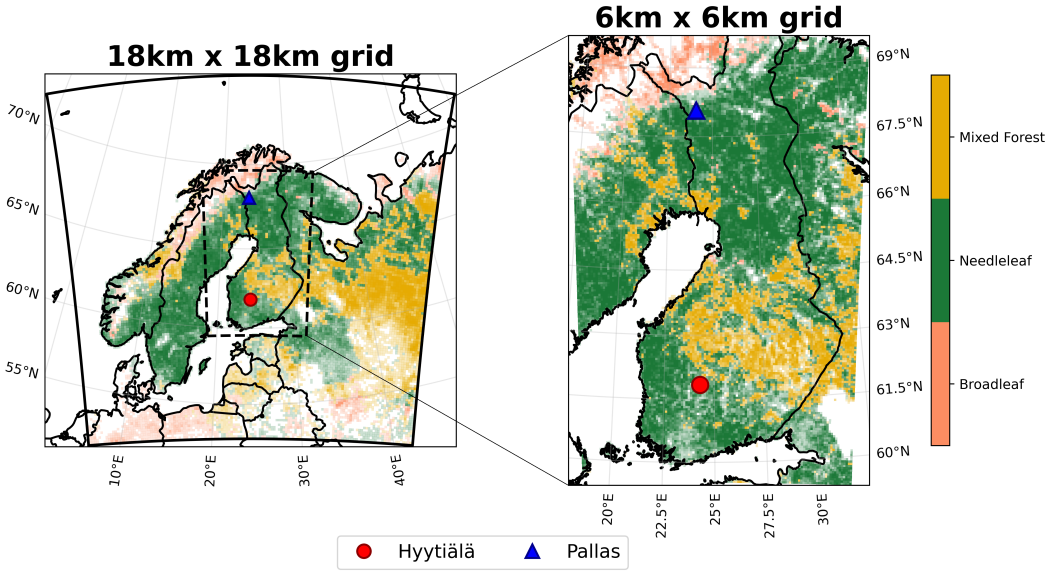

Figure 1. The two model domains: the parent domain with a grid cell size of 18km x 18km, and the nested domain with a grid cell size of 6km x 6km. The black line on the parent domain indicates the boundary of the domain, while black dashed line indicates the position of the nested domain. The red circle denotes the location of the SMEAR-II station in Hyytiälä, while the blue triangle denotes the location of the Sammaltunturi station in Pallas. The color indicates the forest type in each grid cell, while the shading represents the percentage of the cell covered by forest based on USGS land cover data.

temporal resolution of 6 hours and a horizontal resolution of 1°, with the coarse domain nudged toward the reanalysis fields to maintain consistency.

Atmospheric composition boundary and initial conditions were retrieved from climatological simulations of LMDz-INCA3 (Hauglustaine et al., 2014) for gaseous and particulate species and GOCART (Chin et al., 2002) for dust concentrations.

Yearly anthropogenic emissions of carbon monoxide (CO), ammonia (NH_3), non-methane volatile organic compounds (NMVOCs), nitrogen oxides (NOx), particulate matter (PM_{10} and $PM_{2.5}$), and sulfur dioxide (SO_2) were retrieved by the CAMS-REG version 6.1 dataset (Kuenen et al., 2022) at a 0.05°× 0.1° grid resolution. These emissions were distributed hourly across the study periods using temporal profiles derived from the EMEP MSC-W model (Simpson et al., 2012).

Biogenic emissions were calculated using the MEGANv2.1 algorithm, which is automatically integrated into the CHIMERE model. This version provides pre-calculated EFs for isoprene (C_5H_8), monoterpenes (divided in α-pinene, β-pinene, limonene, ocimene), humulene and β-caryophyllene with a horizontal resolution of 0.008°×0.008°. Additionally, sensitivity simulations were conducted in which the EFs for isoprene were recalculated using the more recent MEGANv3.2. Further details on this are provided in Section 2.2.

https://doi.org/10.5194/egusphere-2026-352
Preprint. Discussion started: 13 February 2026

2.1.2 Sensitivity simulations

In addition to the baseline simulation, we conducted three sensitivity simulations aimed at improving the estimates of isoprene emissions and concentrations in the model. In the first sensitivity simulation, MEGANv3.2, without any additional modification of the inputs, was used to calculate the EFs for isoprene. The second sensitivity simulation introduced new isoprene EFs calculated with MEGANv3.2, incorporating domain-specific tree cover, tree species distribution, and species-specific EFs (more details are provided in Section 2.2). In the final sensitivity simulation built upon the second, we added a canopy correction based on the approach introduced by Cholakian et al. (2022) to account for the effects of forest canopy on dispersion (further details are provided in the supplementary material). This correction was required because WRF-CHIMERE does not explicitly represent canopy-induced effects on mixing and dispersion, which can lead to biases in simulated BVOC concentrations and their evaluation against observations. Table 1 summarizes the main characteristics of each simulation.

Table 1. Summary of the modification between each simulation. The "Emission factor" column refers to which version of MEGAN has been used to calculate the EF. The "Tree cover + speciation" column indicates if updated tree cover and species distribution has been taken into account or not. The "Canopy correction" column shows which simulation includes the canopy correction.

Simulation name	Emission factor	Tree cover + speciation	Canopy correction
Baseline	MEGAN2.1	Not included	Not included
MEG3	MEGAN3.2	Not included	Not included
MEG3-UPD	MEGAN3.2	Included	Not included
MEG3-UPD-CC	MEGAN3.2	Included	Included

2.2 Isoprene emission factor

To begin, we would like to clarify the terminology used throughout this text, as EF can refer to different concepts. When we use the general term EF, we are referring specifically to the ecosystem level EF of a given grid cell, which is used in the MEGANv2.1 algorithm to calculate actual emissions. To differentiate this from the EF associated with a specific tree species, we will consistently use the term "species-specific EF" when referring to the latter.

Since the MEGANv2.1 algorithm is already integrated into CHIMERE, here we use the MEGANv3.2 EF processor (MEGEFP) only to calculate updated EFs for isoprene. These updated EFs, based on domain-specific vegetation data, were then used as input for the MEGANv2.1 algorithm within CHIMERE. This means that, in this study, all the differences in the final emissions result from modifications to the EFs, not from changes in the activity-factor calculation.

The MEGEFP assigns distinct ecotypes to different regions. For each ecotype, specific tree species are assigned along with their species-specific EF and relative abundances. However, most ecotypes classify trees into two categories only: needleleaf and broadleaf. Although each ecotype includes an ecotype-specific needleleaf and broadleaf class, each with its own species-specific EF, this approach is not fully representative of reality. For example, *Picea abies* (Norway spruce) has a species-specific

https://doi.org/10.5194/egusphere-2026-352
Preprint. Discussion started: 13 February 2026

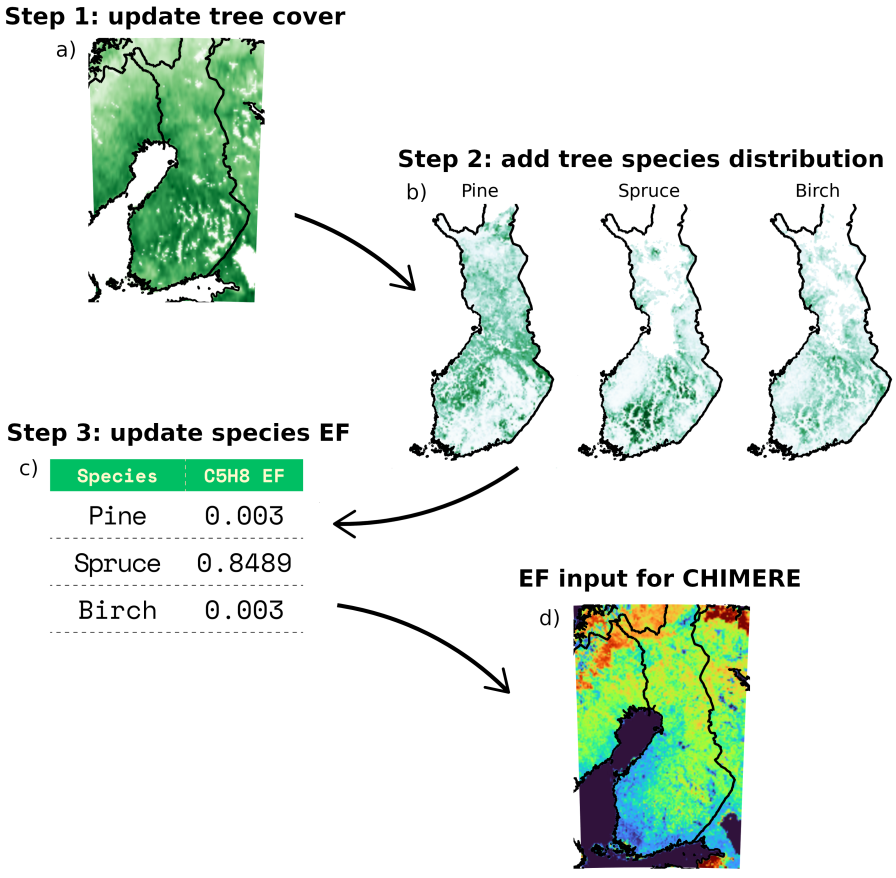

Figure 2. Schematic of the isoprene EF calculation. The scheme shows only the input to the MEGAN3 EF processor that have been modified in this study. These modifications include updating the tree cover percentage (a), the tree species distribution (b), and the species-specific emission factors for isoprene (in units of nanomoles m^{-2} s^{-1} LAI^{-1}) (c). The final output is the gridded isoprene EF (d), which can be used as input for the MEGAN version integrated within the CHIMERE model.

isoprene EF at least one order of magnitude bigger than that of *Pinus sylvestris* (Scots pine) (Lindfors and Laurila, 2000; Tarvainen et al., 2005; Hakola et al., 2023), despite both being classified as needleleaf trees and found in boreal forests.

To improve the accuracy of the EFs, we retrieved high-resolution data on tree cover, tree species distribution, and tree species-specific EF tailored to Finland. This data was then used to update the MEGEFP inputs, allowing for more regionally representative calculations of isoprene emissions. Specifically, this process consists of three main steps (a schematic is shown in Figure 2). In the first step, tree cover data for the year 2019 were retrieved from the Natural Resources Institute Finland (LUKE) website (https://kartta.luke.fi, last access: 20 January 2026) and updated into MEGEFP. During the second step, we retrieved from the same website information about the spatial distribution of three main tree species present in Finland (Scots pine, Norway spruce, and Silver birch), which together account for 97% of all trees. To implement these data in MEGEFP, we

https://doi.org/10.5194/egusphere-2026-352
Preprint. Discussion started: 13 February 2026

utilized its functionality that allows for the definition of multiple ecotypes within the same grid cell, along with the assignment of the percentage of the grid cell covered by each ecotype. Accordingly, we defined three new mono-species ecotypes and assigned the relative percentage of each ecotype based on the retrieved data. This method allows us to include the spatial distribution information for the different tree species in the model, with a high spatial resolution. An alternative, simpler implementation of the second step was also tested. In this version, the original ecotype spatial distribution was retained, and we assumed a uniform distribution of 50% Scots pine, 30% Norway spruce, and 20% Silver birch across the entire ecotype. These percentages represent roughly the average tree species abundance in Finland. This "simple" version was compared to the previous "advanced" version only in terms of the final EFs grid and was not used as input for emissions calculation within CHIMERE. This simplified version was tested because detailed information on tree species distribution is often unavailable in many regions. In such cases, step 2 cannot be implemented, making an alternative approach necessary. Comparing the simplified and advanced versions allows us to quantify the differences, and thus the uncertainties, introduced by assuming a uniform species distribution. In the final step, species-specific isoprene EFs for Scots pine, Norway spruce, and Silver Birch were retrieved from the literature (Lindfors and Laurila, 2000; Tarvainen et al., 2005; Hakola et al., 2023) and incorporated into the EFs tables of MEGEFP. Specifically, for Norway spruce we used the average value of all the EFs available, while for Scots pine and Silver birch we assigned the minimum value present in MEGANv3.2, as for both species extremely small EFs are reported in Finland.

It is important to note that the EFs calculated by MEGANv3.2 represent the leaf-level EF with units of nanomoles m^{-2} s^{-1} LAI^{-1}, rather than at the canopy scale as in previous MEGAN versions, which used units of μg m^{-2} h^{-1} (Silva et al., 2020). This shift from canopy- to leaf-level EFs means that a careful conversion is required when applying MEGANv3.2 derived EFs in MEGANv2.1, specifically, the per LAI basis in MEGANv3.2 must be properly accounted for to ensure consistency across model versions. Unfortunately, there is no exact or formally defined conversion between leaf-level EFs from MEGANv3.2 and canopy-scale EFs used in MEGANv2.1. Therefore, we adopt an approximate approach similar to that of Sindelarova et al. (2022), expressed as:

$$EF_{\mathrm{MEGANv2.1}}[month] = LAI_{\mathrm{std}} \frac{\sum_i^{\mathrm{Ecotype}} f_i \frac{LAI_i[\mathrm{month}]}{LAI_{\mathrm{max}}} EF_{\mathrm{MEGANv3.2},i}}{\sum_i^{\mathrm{Ecotype}} f_i LAI_i[\mathrm{month}]} \quad (1)$$

where f is a fraction of a grid cell covered by a specific PFT. Because MEGANv3.2 includes only a single ecotype over Finland, Equation (1) simplifies to:

$$EF_{\mathrm{MEGANv2.1}} = \frac{LAI_{\mathrm{std}}}{LAI_{\mathrm{max}}} EF_{\mathrm{MEGANv3.2}} \quad (2)$$

where LAI_{std} is set to 5 $m^2 m^{-2}$. Over Finland, LAI_{max} can be choose between 4 and 5 $m^2 m^{-2}$; in this study, a value of 5 $m^2 m^{-2}$ was adopted.

2.3 FLEXPART

The FLEXible PARTicle dispersion model (FLEXPART) is a Lagrangian model used to simulate both the forward and backward dispersion of particles. In this study, we used WRF-FLEXPART version 3.3.2 (Brioude et al., 2013) in backward mode

https://doi.org/10.5194/egusphere-2026-352
Preprint. Discussion started: 13 February 2026

to trace air-mass origins arriving at Hyytiälä. Simulations were driven by meteorological data generated from the WRF simulations (the same used for the CHIMERE simulations), with a temporal resolution of 20 minutes.

The FLEXPART model was configured with one domain matching the resolution and region covered by the outermost domain of the WRF-CHIMERE simulations, with a resolution of 18 × 18 km^2. This domain was designed to capture long-range transport processes. The simulation was setup with 12 vertical levels extending from the surface to 9000 meters above ground level. The layer thickness follows a pseudo-exponential distribution, with finer resolution (50 meter) near the surface and progressively increasing layer depth with altitude.

During the study period, we released 10000 particles per hour from Hyytiälä and tracked their back trajectories over 72 hours. The passive tracer particles were emitted from altitudes ranging from 0 to 100 meters above ground level. The output of FLEXPART in backward mode is the Source-Receptor Relationship (SRR), expressed in units of seconds, which can be interpreted as a proxy of the time the particles spent in each grid cell.

To investigate the impact of air mass history on measured and modelled OA concentrations at Hyytiälä, and to better understand potential sources of bias, we combined OA time series from Hyytiälä with FLEXPART output. Specifically, we calculated the Source Region Contribution (SRC) as described in Bettineschi et al. (2025). Given a simulation domain Ω, containing a simulation time (t), height (h), longitude (x) and latitude (y) as coordinates, and an air mass arrival time (τ), the SRC was calculated assigning the OA concentration/bias recorded during τ, to all the (x, y) grid points intercepted by the air mass (at any height) in the 72 hours prior the release and doing a sum over all the releases, then for each (x, y) pair this value is divided by the number of trajectories that have been intercepted by the given (x, y) grid point. This can be mathematically described by the following equations:

$$\mathrm{SRC}(x,y) = \frac{\sum_\tau \delta(\tau;x,y)\cdot[\mathrm{OA}](\tau)}{\sum_\tau \delta(\tau;x,y)} \tag{3}$$

$$\delta(x,y,\tau) = \begin{cases} 1 & \text{if } \sum_{(t,h)\in\Omega} \mathrm{SRR}(t,h;x,y,\tau) > 0 \\ 0 & \text{otherwise} \end{cases} \tag{4}$$

The SRC metric in this study was used to compare the source regions of measured OA versus modelled OA, this can provide information on whether the model has stronger bias when air masses arrive from a specific region, or if the bias is independent of air mass origin.

Additionally, to further understand the relationship between air masses and OA, we adapted the concept of Air Mass Exposure (AME), as introduced by Hakala et al. (2022). AME calculations combine FLEXPART output with two-dimensional fields (e.g., emissions fields or population density) to determine when air masses were exposed to emissions from different pollutants. Here, we modified the AME calculation by integrating the FLEXPART output with the three-dimensional emissions (i.e., including also the time dimensions) calculated by MEGAN. For each release event, we calculated the AME to monoterpenes emissions according the following equation:

https://doi.org/10.5194/egusphere-2026-352
Preprint. Discussion started: 13 February 2026

$$\mathrm{AME}(\tau) = \sum_{(t,x,y)\in\Omega} \mathrm{SRR}_{500}(t,x,y;\tau) \cdot [\mathrm{Monoterpenes}](t,x,y) \tag{5}$$

$$\mathrm{SRR}_{500}(t,x,y,\tau) = \sum_{h=0}^{500m} \mathrm{SRR}(h;t,x,y,\tau) \tag{6}$$

2.4 Observational data

A diverse set of observational data was used to evaluate the different simulations. Temperature and wind speed measurements from Hyytiälä (see Figure 1) were obtained from the https://smear.avaa.csc.fi website (last access: 20 January 2026) (Junninen et al., 2009) for the entire simulation period. These observations are available at various heights, and in this study, we used all data available within the 2 to 125 meter range.

Ecosystem level BVOCs fluxes from Hyytiälä are used in this study to evaluate the simulated emissions. The BVOC fluxes used here are measured using the surface-layer-profile method with a proton transfer reaction mass spectrometer (PTR-MS) (Rantala et al., 2014), the systematic error of this technique is estimated to be around 10%.

Ground level BVOCs concentrations from Hyytiälä were also retrieved from the https://smear.avaa.csc.fi website (Junninen et al., 2009). Additionally, isoprene concentration from Pallas (see Figure 1) at ground level were retrieved from the EBAS website (https://ebas.nilu.no, last access: 20 January 2026).

OA concentrations from Hyytiälä are measured with a Aerosol Chemical Speciation Monitor (ACSM), as describe by Heikkinen et al. (2020).

3 Results

3.1 Meteorological evaluation

Meteorological conditions play a fundamental role in the simulation of BVOCs emissions and the following aerosol formations and transportation processes, it is thus important to asses whether the main meteorological variables are simulated correctly or not. Figure 3 reports an evaluation of the model performance in relation to temperature and wind speed. The comparison of the vertical profile of average temperature (Figure 3a) shows that the model is in good agreement with the observations, with a small constant underestimation at all heights between 4 to 125 meters above ground level. Similarly, the 2 meters hourly temperature (Figure 3c) is in good agreement across the whole temperature range recorded, which spans roughly 30°C, despite a mean underestimation of 0.74°C in the model. This underestimation occurs mainly during nighttime hours, as shown in the diurnal cycle reported in the supplementary material (Figure S1). Similar cold biases during nighttime have been reported before in several studies (Holtslag et al., 2013; García-Díez et al., 2013; Ciarelli et al., 2024), and it is thought to be caused by excessive vertical mixing in the model during stable boundary layer conditions.

https://doi.org/10.5194/egusphere-2026-352
Preprint. Discussion started: 13 February 2026

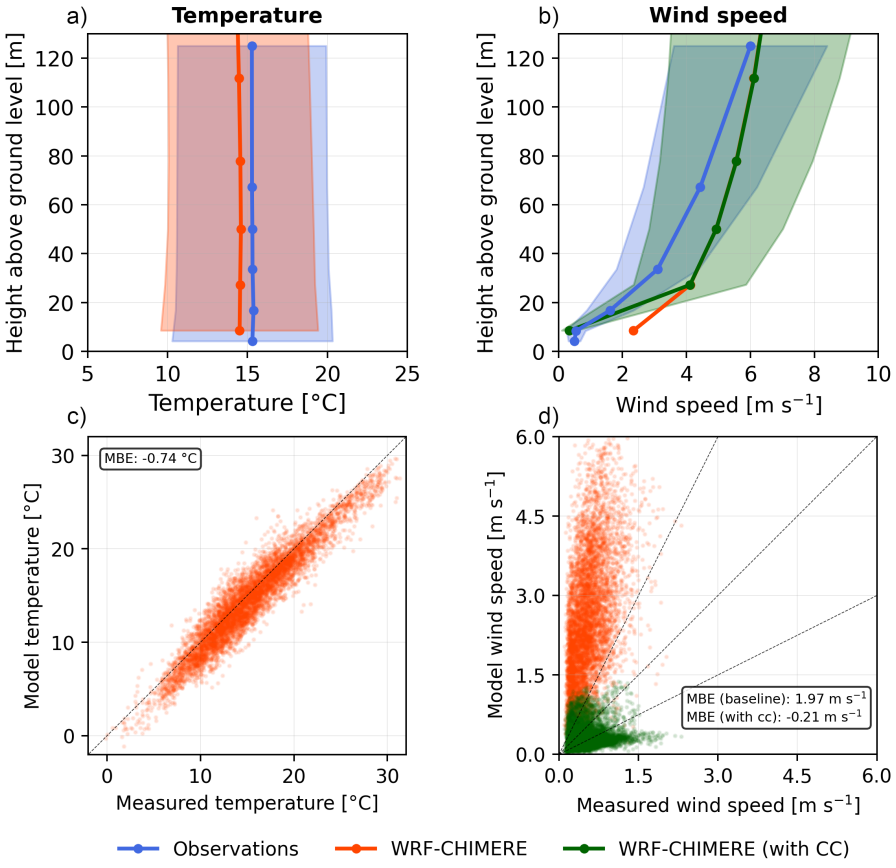

Figure 3. Vertical profiles of mean temperature (a) and wind speed (b), comparing observation at Hyytiälä, and the nearest grid point in the WRF-CHIMERE simulation. In (b) we also show the WRF-CHIMERE simulation with canopy correction (CC). The dots indicate the height of the measurements or the mid-layer height. The shaded area represents the standard deviation from the mean, not reported for the baseline simulation in (b) for better readability of the plot. Comparison of the measured and modelled 2 meters temperature (c), and wind speed at 8 meters (d). Panel (d) shows the baseline (orange) and canopy correction (green) simulations.

As shown in Figure 3b, the wind speed vertical profiles indicate a strong bias compared to the observations. Specifically, in the baseline simulation, the closer to the ground the bigger the overestimation in the model. This is caused by the absence of a coupled canopy model in CHIMERE, which means it cannot take into account the physical effect of the forest canopy on wind speed. We tested the effect of adding a simple canopy correction acting on the first layer of the model as described in the methods section. Figures 3b and 3d show that the canopy correction significantly improves the performance in the first layer of the model, with the mean bias error (MBE) going from 1.97 m s^{-1} in the baseline simulation to -0.21 m s^{-1} in the simulation with the canopy correction.

https://doi.org/10.5194/egusphere-2026-352
Preprint. Discussion started: 13 February 2026

3.2 Isoprene emission factor

The effects of using different input datasets on the calculation of EFs are presented in this section. Figure 4 shows the individual impact of each modification on isoprene EFs across Finland, compared to the baseline MEGANv3.2 configuration.

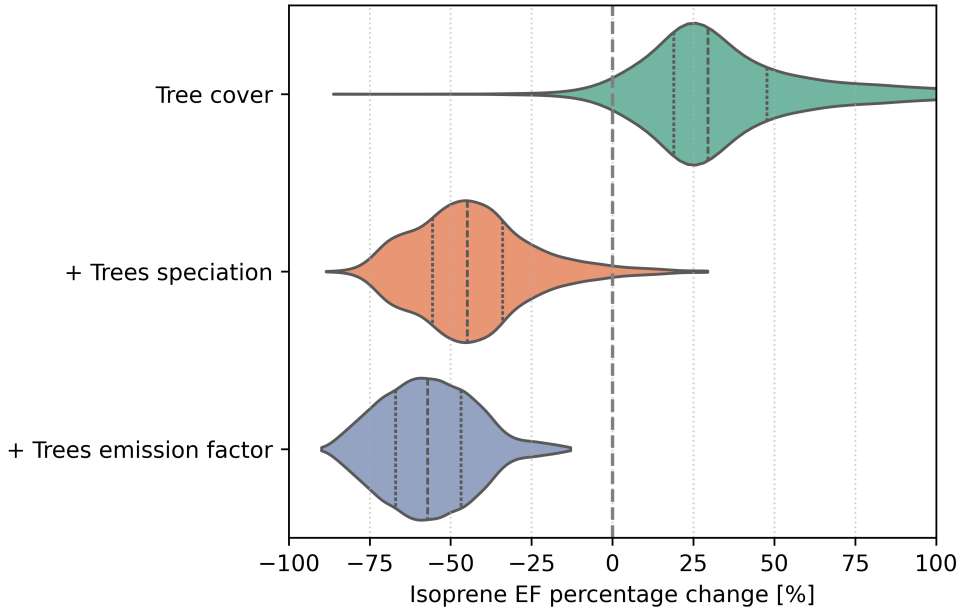

Figure 4. Violin plots of the isoprene emission factor percentage change for the different input modification. The variation is calculated over the whole of Finland in comparison to the base MEGANv3.2 emission factor. The + indicates that the modification is added on top of the previous one. The three modifications correspond to the three step shown in Figure 2. The vertical dotted line inside the violin plot represent the interquartile range and the median value.

Updating the tree cover distribution using high-resolution LUKE data results in a general increase in isoprene EFs across most of Finland. In the majority of grid cells, this increase exceeds 25%. Assuming the LUKE dataset represents the ground truth, this suggests that the tree cover data used in the base MEGANv3.2 version is likely incorrect for Finland and underestimates the actual tree cover.

Adding tree species distribution information on top of the LUKE tree cover leads to a significant decrease in isoprene EFs. This reduction is primarily due to the higher accuracy of the species-specific EFs already present in MEGANv3.2 for Norway spruce, Scots pine, and Silver birch, compared to the more generic species-specific EFs used for the needleleaf/broadleaf "species". This trend continues with the final modification, where only the species-specific EFs are updated. While isoprene EFs still decrease, the variation is smaller than in the previous step. This is because the original species-specific isoprene EFs used in MEGANv3.2 are already reasonably accurate.

https://doi.org/10.5194/egusphere-2026-352
Preprint. Discussion started: 13 February 2026

Adding information about species distribution (i.e., step 2) not only changes the absolute values of the EFs (which could have also been achieved by simply modifying the species-specific isoprene EFs assigned to the needleleaf/broadleaf "species"), but also significantly changes their spatial distribution. This is illustrated in Figure 5, which compares two different approaches

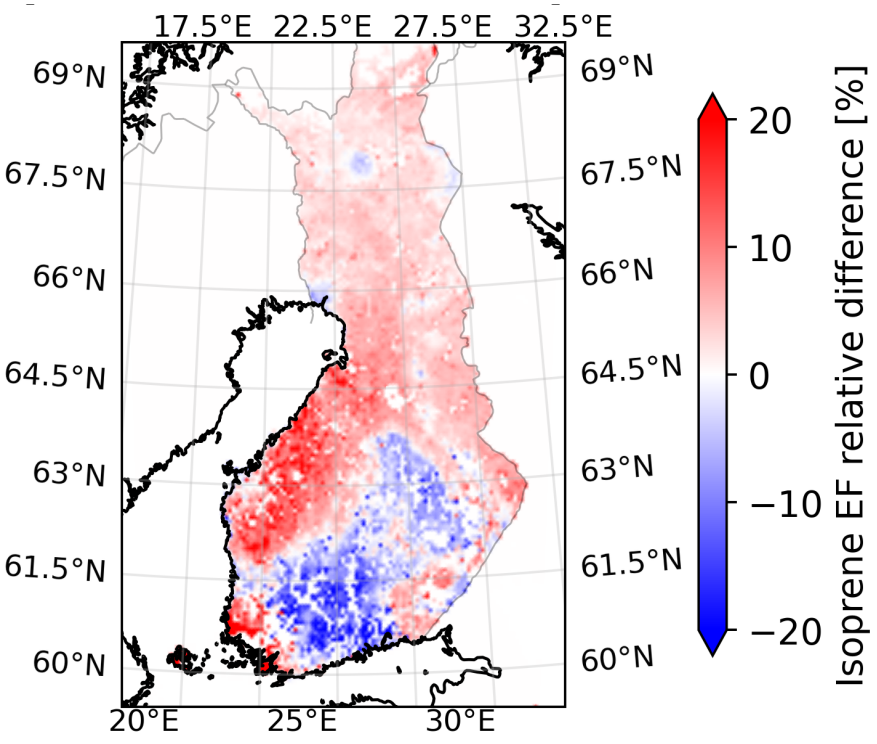

Figure 5. Relative difference between the isoprene emission factors calculated using the "simple" speciation compared the "advanced" speciation. The "advanced" EF have been used as reference.

used in step 2. Assuming a uniform species distribution ("simple" speciation) results in a relative difference in isoprene EFs ranging approximately from -20% to +20%, compared to using a more detailed species distribution ("advanced" speciation). These differences are primarily driven by the distribution of Norway Spruce (see Figure 2), the main isoprene emitter in Finland. In regions with a high relative abundance of Norway spruce, the "simple" speciation approach underestimates isoprene EFs (as shown by the blue areas in Figure 5). The opposite occurs in areas where Scots pine dominates, leading to an overestimation of EFs using the simplified approach.

3.3 Isoprene emission

The effects of using the new isoprene EFs, including all the updated inputs, on modelled isoprene emissions is presented in this section. Figure 6a compares the observed average diurnal cycle of isoprene emissions during summer at the Hyytiälä site with modelled isoprene diurnal emissions from three simulations, each using a different set of EFs. The baseline simulation, which

https://doi.org/10.5194/egusphere-2026-352
Preprint. Discussion started: 13 February 2026

uses the pre-calculated EFs from MEGANv2.1, greatly overestimates isoprene emissions, consistent with previous findings (Jiang et al., 2019; Cholakian et al., 2022; Zhao et al., 2024; Ciarelli et al., 2024). The MEG3 simulation (see Table 1), which uses EFs calculated with the default version of MEGANv3.2, reduces this overestimation by roughly a factor of two. However, despite this improvement, the emissions remain overestimated. The MEG3-UPD simulation, which uses EFs calculated with MEGANv3.2 incorporating all the updated inputs, shows the best performance, with modelled emissions closely matching observations, despite a slight underestimation.

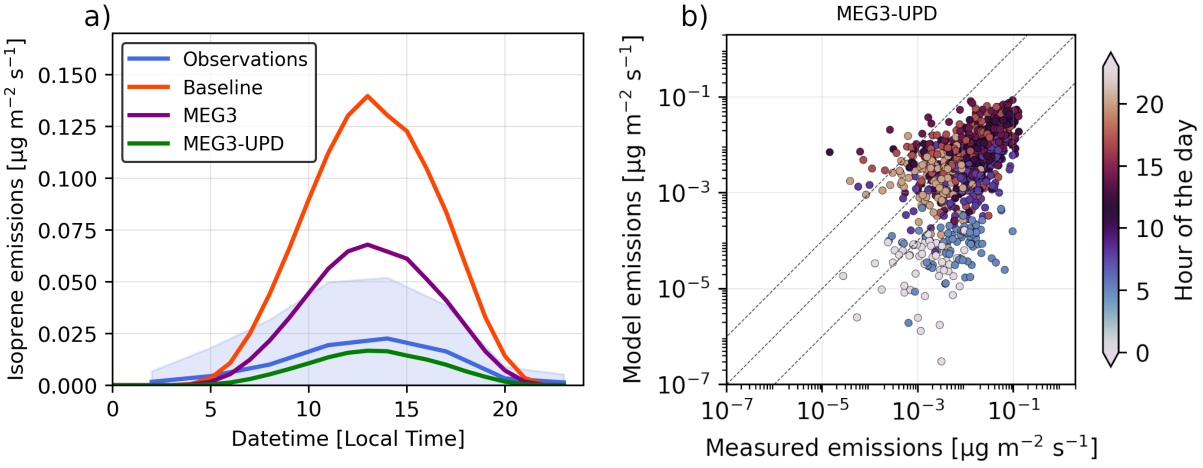

Figure 6. (a) Diurnal variation of observed and WRF-CHIMERE modelled isoprene emissions at Hyytiälä. The mean (solid lines) is reported for observations and all the simulations with different emissions, while the standard deviation (shaded area) is reported only for the observations for better visibility. (b) Scatter plot comparing measured and model-predicted hourly isoprene emissions in log scale. Only the MEG3-UPD simulation is showed. The MBE is displayed in the upper left corner. The dashed lines represents the 10:1, 1:1, and 1:10 agreement between observations and model predictions.

Figure 6b provides a more detailed comparison between the observations and the final simulation. The vast majority of hourly data (79%) fall within an order of magnitude of the observations. A cluster of points, however, shows underestimations greater than a factor of ten, these correspond mostly to night-time. Possible explanations include: (i) the underestimation may be driven by a bias in the simulated diurnal temperature cycle. As mentioned earlier, the model underestimates temperature during night, which could lead to lower simulated isoprene emissions; (ii) the bias could arise from the measurements technique, as during night some isoprene emitted the day before is trapped inside the canopy, during sunrise (in Hyytiälä during summer as early as 3AM local time) with the development of the boundary layer some of this isoprene can be transported upwards and detected as a flux. In other words, since the observations measure ecosystem level fluxes, the direct comparison with emissions might not always be possible. However, if this explanation is correct, it accounts only for a subset of the underestimated points, namely the blue points, which correspond roughly to the sunrise hours.

In Figure 7, the spatial distribution of isoprene emissions from the MEG3-UPD simulation is compared with those from the CAMS-GLOB-BIOv3.1 (CAMS-BIO hereafter) dataset, which has a spatial resolution of 0.25x0.25°, and also use MEGANv2.1

https://doi.org/10.5194/egusphere-2026-352
Preprint. Discussion started: 13 February 2026

(Sindelarova et al., 2022). This dataset is widely used for global and regional modelling and also includes updated isoprene emissions over Europe. Overall, the two datasets show the same order of magnitude over many areas. The largest differences arise in the spatial patterns: CAMS-BIO shows higher emissions in southwestern Finland and in some areas of Lapland compared to MEG3-UPD. Furthermore, the CAMS-BIO dataset does not capture the "high" emission area associated with the high abundance of Norway Spruce, and it underestimates emissions in most of the domain.

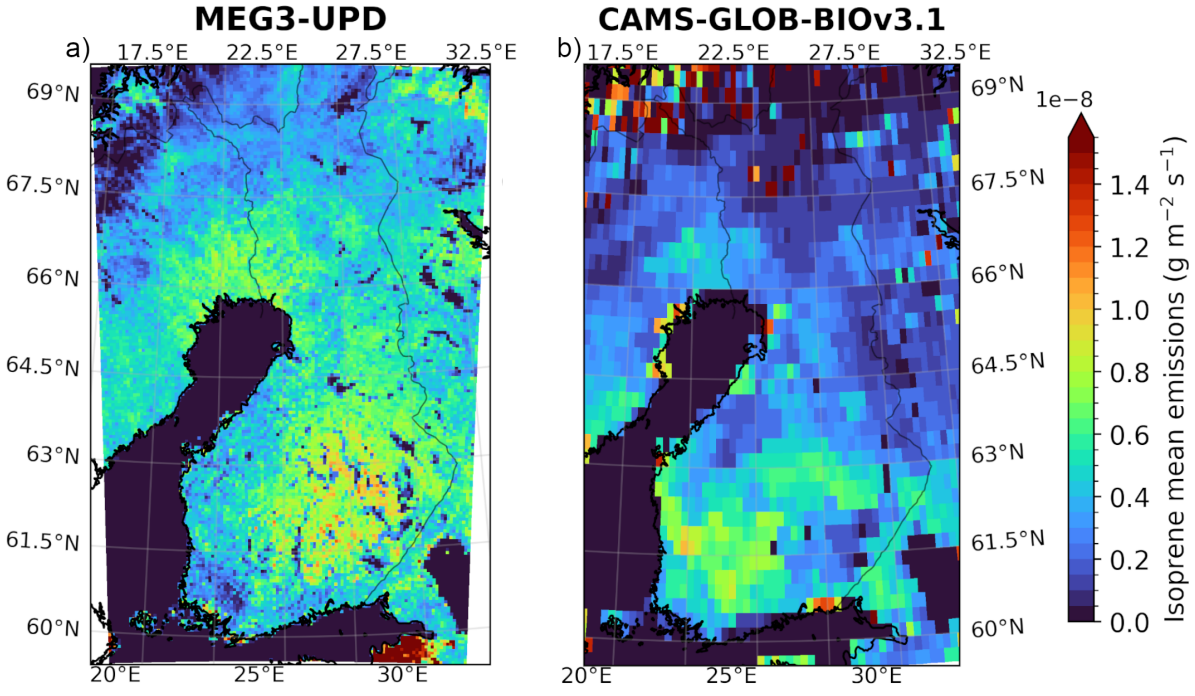

Figure 7. Comparison between the updated isoprene emission used in this study (a) and the CAMS-GLOB-BIOv3.1 dataset (b). Both represent only summer emission during 2017, 2018 and 2019.

3.4 BVOCs concentrations

This section presents the evaluation of all simulations with respect to BVOCs concentrations. Specifically, for each simulation, we compared concentrations of isoprene, monoterpenes, methanol, and acetone with observations from Hyytiälä. In addition, isoprene concentrations were also compared with observations from Pallas.

As shown in Figure 8(a-d), in Hyytiälä the comparison of isoprene concentrations follows a pattern similar to the emissions, as expected: concentrations are greatly overestimated in the baseline simulation, improved by roughly a factor of two in the MEG3 simulation, and further reduced in the MEG3-UPD simulation. Interestingly, the MEG3 simulation yields the lowest MBE across all simulations. We attribute this to a double bias compensation, where excessive emissions cause overestimation, while the absence of a canopy correction leads to underestimation. This interpretation is supported by the MEG3-UPD-CC

https://doi.org/10.5194/egusphere-2026-352
Preprint. Discussion started: 13 February 2026

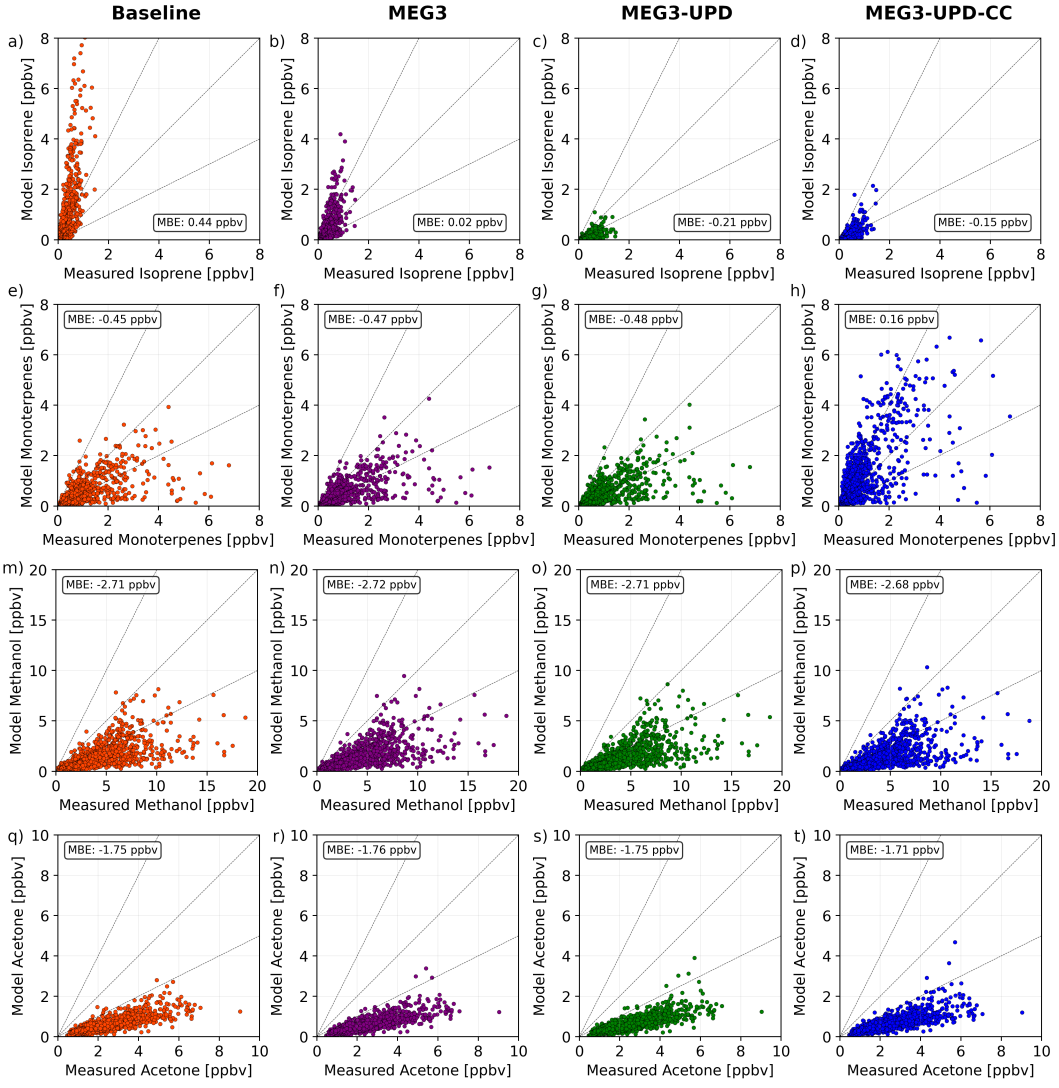

Figure 8. Scatter plot comparing measured and model-predicted concentrations for isoprene (panels a-d), monoterpenes (panels e-h), methanol (panels m-p), and acetone (panels q-t) at Hyytiälä, under the baseline simulation and all sensitivity simulations (MEG3, MEG3-UPD, and MEG3-UPD-CC). Each panel represents a specific combination of compound and simulation, with the MBE indicated in the corner of each subplot. The dashed lines represent the 2:1, 1:1, and 1:2 agreements between observations and model predictions.

320 results (panel d), which show that including a canopy correction increases isoprene concentrations at ground level. Similar results are found at Pallas (Figure 9), although in this case the MEG3-UPD simulation has the lowest MBE, closely followed by MEG3-UPD-CC. This confirms the good performance of the updated emissions, even in an environment (tundra) that is significantly different from the Hyytiälä pine forest. Additionally, in Pallas, the canopy correction has a smaller effect if compared to Hyytiälä, as Pallas is not located inside a forest canopy.

https://doi.org/10.5194/egusphere-2026-352
Preprint. Discussion started: 13 February 2026

Figure 8(e–h) presents the same comparison for monoterpenes. Although monoterpenes emissions were not modified, it is interesting to note that monoterpenes concentrations decrease slightly as isoprene decreases. While the effect is very small, this is consistent with the understanding that isoprene can effectively scavenge OH radicals, reducing their availability to react with monoterpenes. As a consequence, lower isoprene levels translate into more OH available for monoterpenes oxidation, resulting in higher monoterpenes sink. The results also show that the canopy correction has a notable influence on monoterpenes concentrations, similar to its effect on isoprene. Overall, monoterpenes concentrations are more scattered than those of the other BVOCs, suggesting greater complexity in monoterpenes modelling.

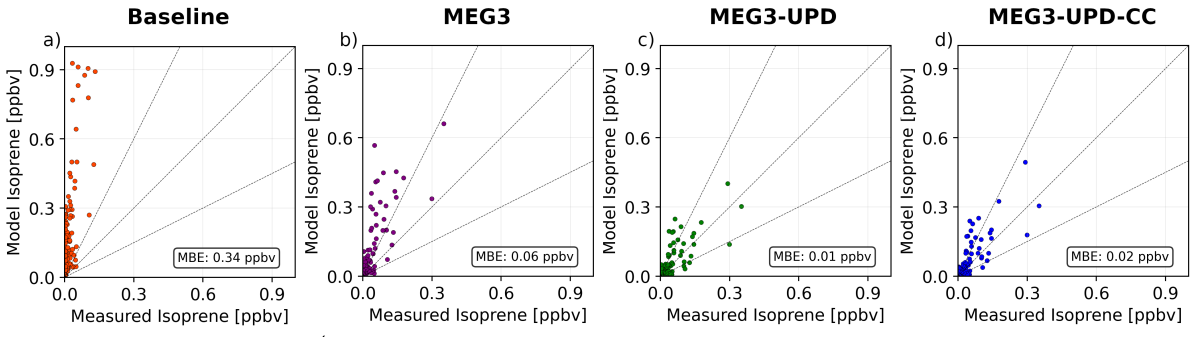

Figure 9. Scatter plot comparing measured and model-predicted concentrations for isoprene at the Pallas station under the baseline simulation and all sensitivity simulations (MEG3, MEG3-UPD, and MEG3-UPD-CC). The MBE indicated in the corner of each subplot. The dashed lines represent the 2:1, 1:1, and 1:2 agreements between observations and model predictions.

Figure 8(m–t) shows the same comparison for methanol and acetone. Similar to monoterpenes, emissions of these compounds were not modified, resulting in only very small predicted changes across the simulations with only isoprene emissions modified. Interestingly, for both methanol and acetone, the canopy correction has a much smaller effect compared to its impact on isoprene or monoterpenes. This is likely because methanol and acetone have significantly longer atmospheric lifetimes than isoprene or monoterpenes. As a result, they are more evenly mixed in the atmosphere and more influenced by regional transport rather than local transport processes. Additionally, although the MBE for methanol and acetone is larger than for monoterpenes, the data points are less scattered. This suggests that emissions of methanol and acetone are likely underestimated, but their atmospheric behavior is simpler to model. A part of this under-prediction of emissions can be due to missing forest floor emissions as well as missing wetlands emissions, as both have been shown to be a significant source of methanol and acetone in the boreal region (Holst et al., 2010; Mäki et al., 2019).

3.5 Canopy correction effect on vertical transport of BVOCs

In this section, we analyze in more detail the effects of the canopy correction on the vertical transport of isoprene and monoterpenes by comparing the MEG3-UPD and the MEG3-UPD-CC simulations. Figure 10 (panels a–d) shows that the impact of the canopy correction depends both on time of day and compound considered.

https://doi.org/10.5194/egusphere-2026-352
Preprint. Discussion started: 13 February 2026

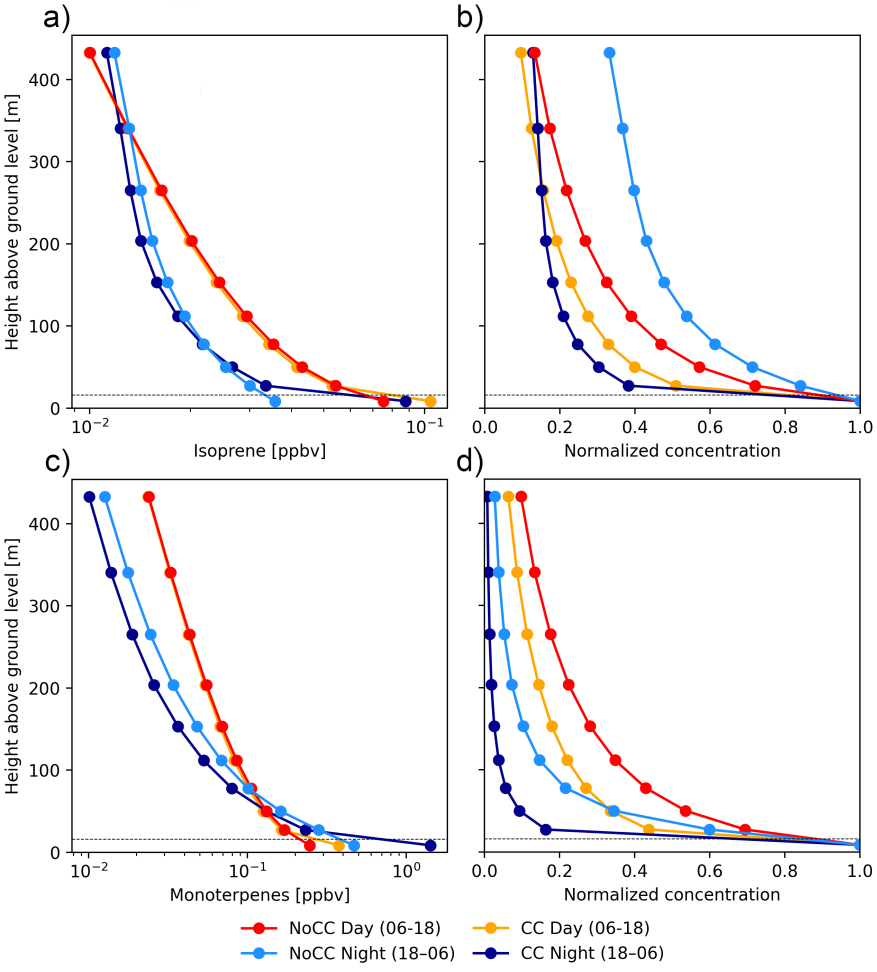

Figure 10. Average vertical profiles of isoprene (a–b) and monoterpenes (c–d) during the daytime (06:00–18:00 local time) and nighttime (18:00–06:00 local time). In b and d the mixing ratios are normalized by the respective average value inside the canopy. The horizontal dashed line represents the average canopy height in Hyytiälä. Only the first ten layers of the model are shown.

Overall, the canopy correction has the largest effect during nighttime. For both isoprene and monoterpenes, canopy correction leads to substantially higher concentrations inside the canopy at night compared to the MEG3-UPD simulation. For monoterpenes this is the result of the nighttime emissions which accumulate inside the forest canopy more efficiently than without canopy correction; this can be seen by looking at the difference between in-canopy concentrations during daytime and nighttime, with and without the canopy correction. For isoprene this is just the result of the lower dispersion, as isoprene emissions are virtually zero during nighttime. This can be seen by the fact that during nighttime the concentrations are lower than during daytime. During daytime, however, the canopy correction effect is limited to within the canopy, while concentrations above the canopy remain largely unaffected; this suggests that during daytime other processes (e.g., oxidation) have a stronger

https://doi.org/10.5194/egusphere-2026-352
Preprint. Discussion started: 13 February 2026

effect on concentrations above the canopy than vertical transport. Above the canopy, the canopy correction generally causes a slight decrease in nighttime concentrations. For monoterpenes, this reduction is visible immediately above the canopy, whereas for isoprene it only becomes apparent above 80 meters. However, the magnitude of this effect is extremely small.

Figure 10b and d show the vertical profiles normalized to the respective average concentration inside the canopy. This normalization serves as a diagnostic of the fraction of the canopy-level concentration that reaches a given altitude (i.e. how efficiently each compound is transported upward). For monoterpenes we can see that both with and without the canopy correction, the relative vertical transport is higher during daytime, as expected due to higher mixing during daytime. However, isoprene shows a different pattern, with higher relative vertical transport during daytime with the canopy correction, but higher during nighttime without the canopy correction.

3.6 Organic Aerosol

This section evaluates the OA concentrations simulated by WRF-CHIMERE, highlighting the effects of isoprene emission reductions and canopy correction. We also present the identification of potential sources of bias.

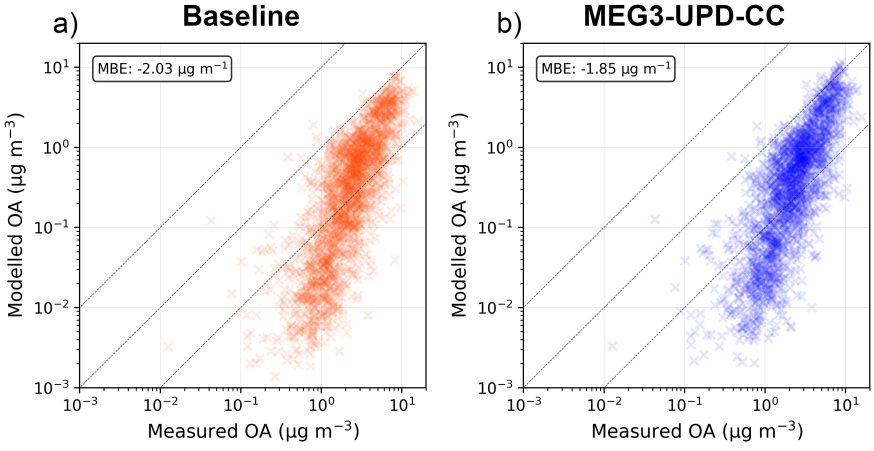

Figure 11. Comparison of OA observations at the Hyytiälä station with modelled OA from the baseline simulation (a) and the MEG3-UPD-CC simulation (b). The MBE for both simulations is indicated in the top-left corner.

Figure 11 shows the comparison of observations in Hyytiälä against the baseline simulation (a) and the MEG3-UPD-CC simulation (b). The simulation that showed the best overall score when considering both isoprene emissions and concentrations (MEG3-UPD-CC) slightly reduced the OA bias when compared to the baseline simulation, however, both simulations show similar pattern with a higher relative underestimation at low OA concentrations, while at higher concentrations the relative error is smaller. This suggests a possible underestimation of the background concentration, as this would have a bigger relative impacts on periods with low concentrations. This missing background is likely due to either missing emissions or too low lateral boundary conditions. From the observations, we estimate the background concentration to be approximately 0.2 μg m^{-3}. This

https://doi.org/10.5194/egusphere-2026-352
Preprint. Discussion started: 13 February 2026

indicates that the missing background can account for only a minor fraction of the model underestimation, particularly at high concentrations. To better identify the sources of bias in the modelled OA, we combined the hourly OA bias ($OA_{measured}$ - OA_{model}) with air-mass back trajectories calculated using FLEXPART. Specifically, by applying the SRC metric, we assessed whether air masses traveling over certain regions are systematically associated with stronger OA underestimation.

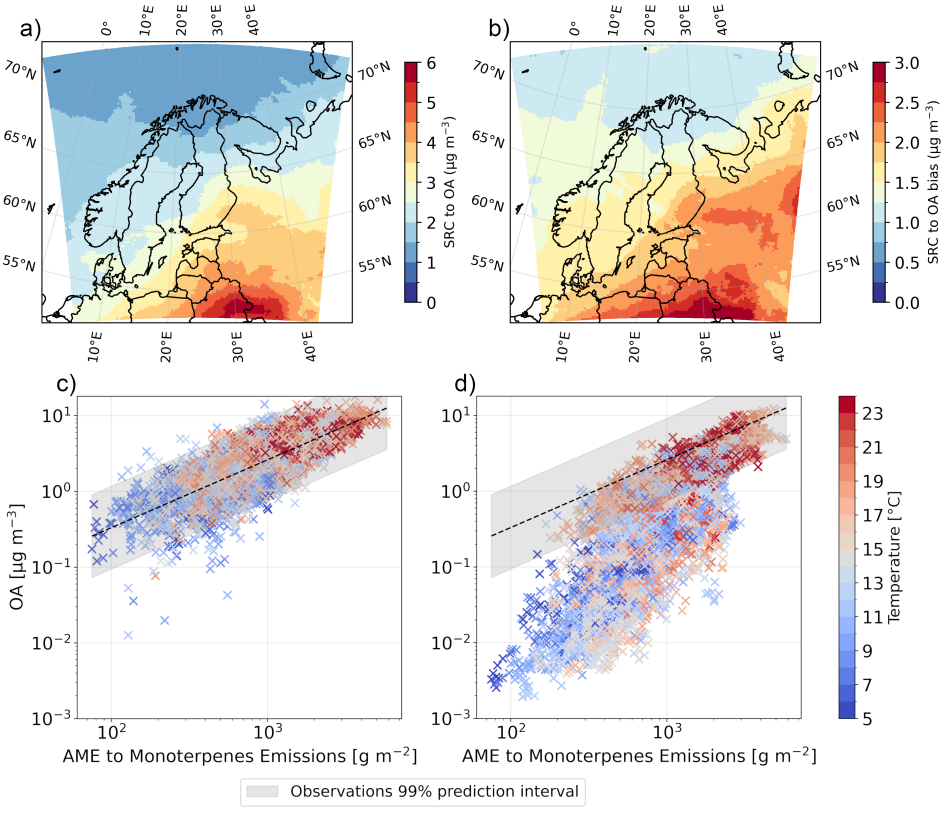

Figure 12. (a) Source region of the OA observed at the Hyytiälä station. The SRC was calculated assigning the OA concentration measured during the release, to all the grid cells intercepted by at least one particle in the 72 hours prior the release. (b) SRC to OA bias (OA_{bias} = $OA_{measured}$ - OA_{model}). Note the difference in the color-bar scale. AME to monoterpenes emissions versus measured OA (c) and modelled OA (d). In both (c) and (d) the 99% prediction interval calculated on observations is shown.

Figure 12a presents the SRC to OA observations, showing that during summer the highest OA concentrations occur when air masses arrive from the south. This finding is consistent with previous studies regarding Hyytiälä, which also identified southerly air masses as more polluted (Riuttanen et al., 2013; Petäjä et al., 2022). Similarly, Figure 12b shows the SRC to OA bias, revealing that the strongest underestimation is linked to air masses arriving from the south and from east. This suggest that the bias could be due to insufficient OA contributions from the southern and eastern boundary conditions of the model domain. Such underestimation could be mitigated either by artificially increasing the boundary concentrations or by expanding

https://doi.org/10.5194/egusphere-2026-352
Preprint. Discussion started: 13 February 2026

the domain size (assuming emissions are accurately represented). To verify this, a sensitivity simulation was conducted in which the first domain was expanded to cover the whole of Europe as shown in Figure S2 in the supplementary material. For computational and storage limit this simulation was performed only for the three summer months of 2018 (the year showing the largest bias). The results revealed only a marginal improvement in model performance, as shown in Figure S3 of the supplementary material, suggesting that the configuration of the first domain accounts for only a minor portion of the overall bias, and it influences the bias only during specific time periods.

As shown in Figure 12c–d, the AME to monoterpene emissions appears to be another factor influencing the model bias. In general, variations in AME explain most of the variability in observed OA ($R^2 = 0.64$). While this is also true for the modelled OA, where variation in the AME explain 62% of the variability ($R^2 = 0.62$), the modelled OA remains consistently lower than the observed OA across all AME levels. This suggests that the BSOA production in the model is under-predicted.

Another potential source of bias is the absence of forest fire emissions in our simulations. Forest fires release substantial amounts of OA and its precursors, which can be transported over long distances. As a result, forest fires can significantly contribute to OA concentrations even in regions far from the fire sources (Ortiz-Amezcua et al., 2017; He et al., 2024; Lee et al., 2025; Olonimoyo et al., 2026). Neglecting these emissions could therefore lead to an underestimation of background OA levels and partially explain the observed discrepancies.

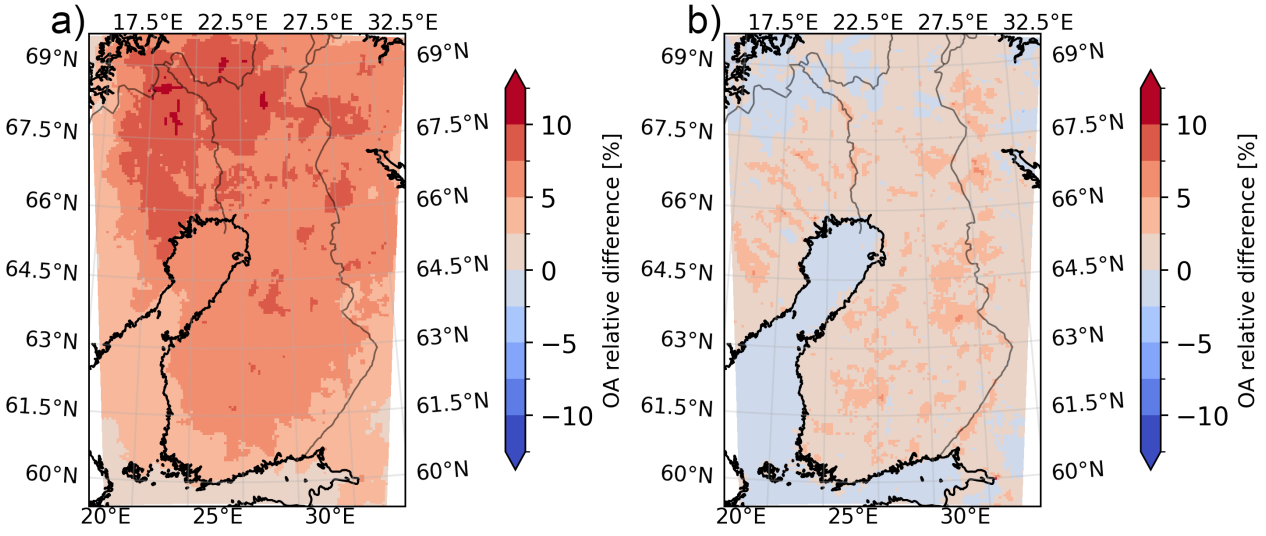

Figure 13. Relative changes in OA concentration. (a) The relative changes are calculated between baseline and MEG3-UPD. (b) The relative changes are calculated between MEG3-UPD and MEG3-UPD-CC.

The effects on the modelled OA concentrations of reducing isoprene emissions and adding the canopy correction are presented in Figure 13a and b. The reduction of isoprene emission resulted in an increase of OA concentrations between 2.5% and 12.5% over most of the domain. This result can be explained by the fact that SOA yields from isoprene are lower compared to

https://doi.org/10.5194/egusphere-2026-352
Preprint. Discussion started: 13 February 2026

monoterpenes, and previous studies have shown that isoprene can effectively scavenge OH radicals, preventing their reaction against other terpenoids, thus limiting the formation of SOA (McFiggans et al., 2019). This reduction in the model is also in agreement with a previous modelling study, Ciarelli et al. (2024) performed a sensitivity simulation removing completely isoprene emissions over Europe and showed that this resulted in a non-negligible (between 10% to 25%) increase in the BSOA mass concentrations over large areas (mostly boreal forests). Activating the canopy correction resulted in a minor effect if compared to the isoprene emissions reduction, with an increase in OA concentrations lower than 5% practically everywhere. Additionally, a minor decrease is visible over the sea, lakes and mountainous regions due to the inhibition of the transport out of the forests.

4 Discussion and recommendations

In this section, we compare our results with previous studies, highlight the new insights gained, and provide recommendations for future research.

Overall, the modifications introduced here led to more realistic isoprene emissions and concentrations, and a reduction in model biases for both BVOCs and OA. At the same time, the analysis also revealed persistent challenges, including the underestimation of OA and the incomplete representation of certain ecosystem sources, such as emissions from forest floor and wetlands.

Our study further develops the work of Cholakian et al. (2022), which studied the influence of domain-specific land-use information on BVOC emissions simulated with MEGANv3.2. The most significant advance in this work compared to Cholakian et al. (2022) is the shift from an ecotype-based approach with constant species distributions within a given ecotype to a high-resolution representation of species distributions in the EFs calculations. In this framework, virtually every grid cell contains a unique tree species composition. Our results show that the spatial distribution of tree species strongly affects the final EFs, with variation in isoprene EFs ranging from -20 to 20% compared to the spatially uniform species distribution case. Additionally, our results show that incorporating information about tree-species can significantly modify EFs relative to cases where MEGAN relies solely on the needleleaf/broadleaf distinction in each ecotype. Because the standard MEGANv3.2 configuration includes species information only for the contiguous United States, this limitation introduces considerable uncertainty in global applications. Future efforts should therefore prioritize the development of comprehensive, species- or at least genera-level, tree distribution datasets at the global scale. On top of that, more extensive measurements of species-specific EFs should be conducted for as many tree species as possible. Expanding the empirical basis of species-specific EFs is essential for reducing model uncertainty and improving the robustness of global and regional biogenic emissions estimates.

Further improvements for future work is the extension of this framework to wetlands, which are widespread across the boreal region yet remain underrepresented in current emission models. High-latitude wetlands are significant sources of BVOCs, including isoprene and terpenes, and their emissions have been shown to be highly sensitive to temperature changes (Vettikkat et al., 2023). This sensitivity underscores the importance of incorporating wetlands into future studies, particularly when

https://doi.org/10.5194/egusphere-2026-352
Preprint. Discussion started: 13 February 2026

investigating climate–biosphere feedbacks such as the interaction between global warming and aerosol formation from natural sources.

The implementation of the canopy correction improved the simulation of in-canopy concentrations, highlighting the strong influence of the forest canopy in regulating near-surface BVOCs levels through its control on vertical mixing and advection. However, its impact on concentrations above the canopy and on regional OA levels was minor. While this may limit its importance for large-scale modelling, a canopy correction remains valuable for accurately simulating BVOCs concentrations inside the canopy, and is therefore crucial when comparing model outputs with in-canopy observations. It should also be noted that the canopy correction applied here was relatively simple, affecting only the first model layer; a more detailed representation that accounts for layers adjacent to the canopy may further enhance model performance.

Despite improved isoprene representation (MBE reduced from 0.44 ppbv in the baseline to -0.15 ppbv with all modifications), mainly due to updated emissions, and improved monoterpene representation (MBE improved from -0.45 ppbv to 0.16 ppbv), largely attributable to the canopy correction, OA concentrations remained underestimated, particularly during episodes of southerly and easterly air-mass transport. Back-trajectories analysis revealed that this bias is partially attributable to underestimated contributions from boundary conditions. Increasing the size of the model domain only partially mitigate this problem. Another factor contributing to the underestimation is the model's insufficient production of BSOA. In particular, OA concentrations in Hyytiälä were found to depend strongly on the degree to which air masses had been exposed to monoterpene emissions during the 72 hours prior their arrival. Across the full range of these exposure levels, the model systematically underestimated the resulting OA, indicating a systematic underproduction of BSOA under the typical conditions found in the boreal region. Numerous factors can contribute to this underproduction. For instance, in the model, the oxidation products of different BVOCs are distributed into four volatility classes based on their C^*, with the lowest C^* of 1 μg m^{-3} corresponding to what is typically defined as semi-volatile organic compounds (SVOCs). However, low-volatility (LVOCs), extremely low-volatility (ELVOCs), and ultralow-volatility (ULVOCs) organic compounds have been shown to be critical for the growth of aerosols to sizes at which SVOCs can effectively condense (Jokinen et al., 2015; Stolzenburg et al., 2023; Dada et al., 2023; Lopez et al., 2025). The absence, or more detailed representation, of LVOCs, ELVOCs, and ULVOCs in the VBS scheme used in this study can therefore lead to two main issues: i) a direct underestimation of condensable gases, resulting in lower BSOA production, and ii) limited growth of freshly nucleated particles, which indirectly reduces BSOA by underestimating the number of particles large enough for SVOCs to condense onto.

Additionally, our results confirm earlier findings that isoprene reduction can increase OA production under certain conditions, due to reduced scavenging of OH radicals and enhanced oxidation of monoterpenes.

Based on these findings, we make the following recommendations for future studies:

- For BVOCs emissions estimation, incorporating high-resolution species distribution information is highly recommended over uniform distribution for each ecotype. If this is not possible, including all the main tree species or genera (with uniform distribution) present in a given ecotype should be preferred over the simple needleleaf/broadleaf classification.

https://doi.org/10.5194/egusphere-2026-352
Preprint. Discussion started: 13 February 2026

- BVOCs emissions from wetlands should be included in future studies, ideally following the same framework presented in this study.
- When performing simulations over domains including forests we recommend to include the forest canopy effect on vertical diffusivity and wind speed. This is especially important when evaluating models with observations inside the canopy, as the absence of a canopy correction would significantly influence the model output in the layers inside the canopy. This has also been noted by Cholakian et al. (2022).
- A more detailed representation of the physicochemical properties of organic compounds should be incorporated. In particular, LVOCs, ELVOCs, and ULVOCs should also be explicitly included in atmospheric models. While few CTMs already account for this process, big uncertainties remain and this will require additional efforts from laboratory studies to better constrain the key reaction pathways and their corresponding yields.

5 Conclusions

In this study we evaluated a regionally customized implementation of MEGAN for boreal forests and assessed its implications for simulated BVOC emissions and SOA formation over Finland. Using updated tree-species distributions, revised species-specific EFs, the study show a significant improvements in isoprene emissions calculation. The updated EFs substantially reduce the long-standing high bias in isoprene emissions over the boreal forest.

The inclusion of the canopy correction on wind speed and vertical mixing improves the representation of BVOCs concentrations within the forest canopy, improving the agreement with in-canopy measurements. Above the canopy, the impact of the canopy correction is limited, indicating that its primary relevance lies in the comparison of in-canopy BVOC observations with models, rather than in regional-scale implications.

Reduced isoprene emissions results in increased OA in large parts of Finland due to decreased competition between isoprene and monoterpenes for OH radical, consistent with previous studies. However, the model continues to underestimate OA even in the best simulation with all the modifications. Back-trajectory analysis shows that the strongest negative biases occur during transport from southern and eastern sectors, which are also associated with higher exposure to monoterpenes emissions. The analysis further reveals that the OA response to monoterpene emissions exposure of the air masses is qualitatively reasonable but systematically underestimated, implying underproduction of BSOA in the model. In this context, a more detailed treatment of the formation and fate of LVOC, ELVOC, and ULVOC species, including their explicit representation in the chemical mechanism and their contribution to condensable mass, could likely improve the model's ability to capture the observed behavior.

Overall, the study identifies three elements important for improved BVOC–aerosol modelling in boreal environments and globally: (i) detailed tree species distribution inputs for the EFs calculation, (ii) representation of canopy effects on mixing processes when confronting in-canopy observations with modelled ones, and (iii) chemical mechanisms capable of forming low-volatility products from monoterpenes, isoprene, and other BVOCs. Progress in these areas, combined with the addition

https://doi.org/10.5194/egusphere-2026-352
Preprint. Discussion started: 13 February 2026

of other BVOCs sources such as wetlands, will be necessary to increase confidence in regional and global assessments of BVOC-driven aerosol–climate interactions.

Data availability. The updated isoprene emission factors for Finland are available at the following link: https://doi.org/10.5281/zenodo.18310397

Author contributions. The study was designed by GC. MB made all the modification related to MEGAN, run all the simulations and analyzed the data. AC provided extensive support in running the WRF-CHIMERE model and preparing the model data. MB prepared the first version of the manuscript. All the co-authors contributed to the discussion and interpretation of the results and the revision of the article.

Competing interests. At least one of the (co-)authors is a member of the editorial board of Atmospheric Chemistry and Physics.

Acknowledgements. This study was supported by the Finnish National Agency For Education (EDUFI Fellowship). The authors wish to acknowledge CSC – IT Center for Science, Finland, for computational resources. Simulations were performed on the Mahti supercomputer (project number: 2008324). ChatGPT (OpenAI's language model) was used to enhance the writing style of this paper. The authors reviewed and revised the AI-modified text and take full responsibility for the content of this publication.

https://doi.org/10.5194/egusphere-2026-352
Preprint. Discussion started: 13 February 2026

References

Arneth, A., Schurgers, G., Lathiere, J., Duhl, T., Beerling, D., Hewitt, C., Martin, M., and Guenther, A.: Global terrestrial isoprene emission models: sensitivity to variability in climate and vegetation, Atmospheric Chemistry and Physics, 11, 8037–8052, https://doi.org/10.5194/acp-11-8037-2011, 2011.

Atkinson, R.: Atmospheric chemistry of VOCs and NOx, Atmospheric environment, 34, 2063–2101, https://doi.org/10.1016/S1352-2310(99)00460-4, 2000.

Bergström, R., Denier Van Der Gon, H., Prévôt, A. S., Yttri, K. E., and Simpson, D.: Modelling of organic aerosols over Europe (2002–2007) using a volatility basis set (VBS) framework: application of different assumptions regarding the formation of secondary organic aerosol, Atmospheric Chemistry and Physics, 12, 8499–8527, https://doi.org/10.5194/acp-12-8499-2012, 2012.

Bessagnet, B., Menut, L., Lapere, R., Couvidat, F., Jaffrezo, J.-L., Mailler, S., Favez, O., Pennel, R., and Siour, G.: High resolution chemistry transport modeling with the on-line CHIMERE-WRF model over the French Alps—analysis of a feedback of surface particulate matter concentrations on mountain meteorology, Atmosphere, 11, 565, https://doi.org/10.3390/atmos11060565, 2020.

Bettineschi, M., Vitali, B., Cholakian, A., Zardi, D., Sinclair, V., Bianchi, F., Mikkola, J., Cristofanelli, P., Marinoni, A., Mazzini, M., et al.: Across land, sea, and mountain: sulphate aerosol sources and transport dynamics over the northern Apennines, Environmental Science: Atmospheres, https://doi.org/10.1039/D5EA00035A, 2025.

Bianchi, F., Kurtén, T., Riva, M., Mohr, C., Rissanen, M. P., Roldin, P., Berndt, T., Crounse, J. D., Wennberg, P. O., Mentel, T. F., et al.: Highly oxygenated organic molecules (HOM) from gas-phase autoxidation involving peroxy radicals: A key contributor to atmospheric aerosol, Chemical reviews, 119, 3472–3509, https://doi.org/10.1021/acs.chemrev.8b00395, 2019.

Brioude, J., Arnold, D., Stohl, A., Cassiani, M., Morton, D., Seibert, P., Angevine, W., Evan, S., Dingwell, A., Fast, J. D., et al.: The Lagrangian particle dispersion model FLEXPART-WRF version 3.1, Geoscientific Model Development, 6, 1889–1904, https://doi.org/10.5194/gmd-6-1889-2013, 2013.

Carter, W. P.: Development of the SAPRC-07 chemical mechanism, Atmospheric Environment, 44, 5324–5335, https://doi.org/10.1016/j.atmosenv.2010.01.026, 2010.

Chin, M., Ginoux, P., Kinne, S., Torres, O., Holben, B. N., Duncan, B. N., Martin, R. V., Logan, J. A., Higurashi, A., and Nakajima, T.: Tropospheric aerosol optical thickness from the GOCART model and comparisons with satellite and Sun photometer measurements, Journal of the atmospheric sciences, 59, 461–483, https://doi.org/10.1175/1520-0469(2002)059<0461:TAOTFT>2.0.CO;2, 2002.

Cholakian, A., Beekmann, M., Colette, A., Coll, I., Siour, G., Sciare, J., Marchand, N., Couvidat, F., Pey, J., Gros, V., et al.: Simulation of fine organic aerosols in the western Mediterranean area during the ChArMEx 2013 summer campaign, Atmospheric chemistry and physics, 18, 7287–7312, https://doi.org/10.5194/acp-18-7287-2018, 2018.

Cholakian, A., Beekmann, M., Siour, G., Coll, I., Cirtog, M., Ormeño, E., Flaud, P.-M., Perraudin, E., and Villenave, E.: Simulation of organic aerosol, its precursors and related oxidants in the Landes pine forest in south-western France: Need to account for domain specific land-use and physical conditions, Atmospheric Chemistry and Physics Discussions, 2022, 1–41, https://doi.org/10.5194/acp-23-3679-2023, 2022.

Ciarelli, G., Theobald, M. R., Vivanco, M. G., Beekmann, M., Aas, W., Andersson, C., Bergström, R., Manders-Groot, A., Couvidat, F., Mircea, M., et al.: Trends of inorganic and organic aerosols and precursor gases in Europe: insights from the EURODELTA multi-model experiment over the 1990–2010 period, Geoscientific Model Development, 12, 4923–4954, https://doi.org/10.5194/gmd-12-4923-2019, 2019.

https://doi.org/10.5194/egusphere-2026-352
Preprint. Discussion started: 13 February 2026

Ciarelli, G., Tahvonen, S., Cholakian, A., Bettineschi, M., Vitali, B., Petäjä, T., and Bianchi, F.: On the formation of biogenic secondary organic aerosol in chemical transport models: an evaluation of the WRF-CHIMERE (v2020r2) model with a focus over the Finnish boreal forest, Geoscientific Model Development, 17, 545–565, https://doi.org/10.5194/gmd-17-545-2024, 2024.

Ciarelli, G., Cholakian, A., Bettineschi, M., Vitali, B., Bessagnet, B., Sinclair, V. A., Mikkola, J., El Haddad, I., Zardi, D., Marinoni, A., et al.: The impact of the Himalayan aerosol factory: results from high resolution numerical modelling of pure biogenic nucleation over the Himalayan valleys, Faraday Discussions, 258, 76–93, https://doi.org/10.1039/D4FD00171K, 2025.

Dada, L., Stolzenburg, D., Simon, M., Fischer, L., Heinritzi, M., Wang, M., Xiao, M., Vogel, A. L., Ahonen, L., Amorim, A., et al.: Role of sesquiterpenes in biogenic new particle formation, Science advances, 9, eadi5297, https://doi.org/10.1126/sciadv.adi5297, 2023.

Dommen, J., Metzger, A., Duplissy, J., Kalberer, M., Alfarra, M. R., Gascho, A., Weingartner, E., Prévôt, A. S., Verheggen, B., and Baltensperger, U.: Laboratory observation of oligomers in the aerosol from isoprene/NOx photooxidation, Geophysical Research Letters, 33, https://doi.org/10.1029/2006GL026523, 2006.

Donahue, N. M., Robinson, A., Stanier, C., and Pandis, S.: Coupled partitioning, dilution, and chemical aging of semivolatile organics, Environmental science & technology, 40, 2635–2643, https://doi.org/10.1021/es052297c, 2006.

Edney, E., Kleindienst, T., Jaoui, M., Lewandowski, M., Offenberg, J., Wang, W., and Claeys, M.: Formation of 2-methyl tetrols and 2-methylglyceric acid in secondary organic aerosol from laboratory irradiated isoprene/NOx/SO2/air mixtures and their detection in ambient PM2. 5 samples collected in the eastern United States, Atmospheric Environment, 39, 5281–5289, https://doi.org/10.1016/j.atmosenv.2005.05.031, 2005.

Ehn, M., Thornton, J. A., Kleist, E., Sipilä, M., Junninen, H., Pullinen, I., Springer, M., Rubach, F., Tillmann, R., Lee, B., et al.: A large source of low-volatility secondary organic aerosol, Nature, 506, 476–479, https://doi.org/10.1038/nature13032, 2014.

Falasca, S. and Curci, G.: Impact of highly reflective materials on meteorology, PM10 and ozone in urban areas: a modeling study with WRF-CHIMERE at high resolution over Milan (Italy), Urban Science, 2, 18, https://doi.org/10.3390/urbansci2010018, 2018.

Fowler, D., Pilegaard, K., Sutton, M. A., Ambus, P., Raivonen, M., Duyzer, J., Simpson, D., Fagerli, H., Fuzzi, S., Schjoerring, J. K., et al.: Atmospheric composition change: ecosystems–atmosphere interactions, Atmospheric Environment, 43, 5193–5267, https://doi.org/10.1016/j.atmosenv.2009.07.068, 2009.

Gao, C., Zhang, X., Xiu, A., Tong, Q., Zhao, H., Zhang, S., Yang, G., Zhang, M., and Xie, S.: Intercomparison of multiple two-way coupled meteorology and air quality models (WRF v4. 1.1–CMAQ v5. 3.1, WRF–Chem v4. 1.1, and WRF v3. 7.1–CHIMERE v2020r1) in eastern China, Geoscientific Model Development, 17, 2471–2492, https://doi.org/10.5194/gmd-17-2471-2024, 2024.

García-Díez, M., Fernández, J., Fita, L., and Yagüe, C.: Seasonal dependence of WRF model biases and sensitivity to PBL schemes over Europe, Quarterly Journal of the Royal Meteorological Society, 139, 501–514, https://doi.org/10.1002/qj.1976, 2013.

Guenther, A., Hewitt, C. N., Erickson, D., Fall, R., Geron, C., Graedel, T., Harley, P., Klinger, L., Lerdau, M., McKay, W., et al.: A global model of natural volatile organic compound emissions, Journal of Geophysical Research: Atmospheres, 100, 8873–8892, https://doi.org/10.1029/94JD02950, 1995.

Guenther, A., Karl, T., Harley, P., Wiedinmyer, C., Palmer, P. I., and Geron, C.: Estimates of global terrestrial isoprene emissions using MEGAN (Model of Emissions of Gases and Aerosols from Nature), Atmospheric Chemistry and Physics, 6, 3181–3210, https://doi.org/10.5194/acp-6-3181-2006, 2006.

Guenther, A., Jiang, X., Heald, C. L., Sakulyanontvittaya, T., Duhl, T. a., Emmons, L., and Wang, X.: The Model of Emissions of Gases and Aerosols from Nature version 2.1 (MEGAN2. 1): an extended and updated framework for modeling biogenic emissions, Geoscientific Model Development, 5, 1471–1492, https://doi.org/10.5194/gmd-5-1471-2012, 2012.

https://doi.org/10.5194/egusphere-2026-352
Preprint. Discussion started: 13 February 2026

Guenther, A., Jiang, X., Shah, T., Huang, L., Kemball-Cook, S., and Yarwood, G.: Model of emissions of gases and aerosol from nature version 3 (MEGAN3) for estimating biogenic emissions, in: Air Pollution Modeling and its Application XXVI 36, pp. 187–192, https://doi.org/10.1007/978-3-030-22055-6_29, 2020.

Hakala, S., Vakkari, V., Bianchi, F., Dada, L., Deng, C., Dällenbach, K., Fu, Y., Jiang, J., Kangasluoma, J., Kujansuu, J., et al.: Observed coupling between air mass history, secondary growth of nucleation mode particles and aerosol pollution levels in Beijing, Environmental science: atmospheres, 2, 146–164, https://doi.org/10.1039/D1EA00089F, 2022.

Hakola, H., Tarvainen, V., Praplan, A. P., Jaars, K., Hemmilä, M., Kulmala, M., Bäck, J., and Hellén, H.: Terpenoid and carbonyl emissions from Norway spruce in Finland during the growing season, Atmospheric Chemistry and Physics, 17, 3357–3370, https://doi.org/10.5194/acp-17-3357-2017, 2017.

Hakola, H., Taipale, D., Praplan, A., Schallhart, S., Thomas, S., Tykkä, T., Helin, A., Bäck, J., and Hellén, H.: Emissions of volatile organic compounds from Norway spruce and potential atmospheric impacts, Frontiers in Forests and Global Change, 6, 1116 414, https://doi.org/10.3389/ffgc.2023.1116414, 2023.

Harrison, S. P., Morfopoulos, C., Dani, K. S., Prentice, I. C., Arneth, A., Atwell, B. J., Barkley, M. P., Leishman, M. R., Loreto, F., Medlyn, B. E., et al.: Volatile isoprenoid emissions from plastid to planet, New Phytologist, 197, 49–57, https://doi.org/10.1111/nph.12021, 2013.

Hauglustaine, D. A., Balkanski, Y., and Schulz, M.: A global model simulation of present and future nitrate aerosols and their direct radiative forcing of climate, Atmospheric Chemistry and Physics, 14, 11 031–11 063, https://doi.org/10.5194/acp-14-11031-2014, 2014.

He, Y., Zhao, B., Wang, S., Valorso, R., Chang, X., Yin, D., Feng, B., Camredon, M., Aumont, B., Dearden, A., et al.: Formation of secondary organic aerosol from wildfire emissions enhanced by long-time ageing, Nature Geoscience, 17, 124–129, https://doi.org/10.1038/s41561-023-01355-4, 2024.

Heikkinen, L., Äijälä, M., Riva, M., Luoma, K., Dällenbach, K., Aalto, J., Aalto, P., Aliaga, D., Aurela, M., Keskinen, H., et al.: Long-term sub-micrometer aerosol chemical composition in the boreal forest: inter-and intra-annual variability, Atmospheric Chemistry and Physics, 20, 3151–3180, https://doi.org/10.5194/acp-20-3151-2020, 2020.

Hoffmann, T., Odum, J. R., Bowman, F., Collins, D., Klockow, D., Flagan, R. C., and Seinfeld, J. H.: Formation of organic aerosols from the oxidation of biogenic hydrocarbons, Journal of Atmospheric Chemistry, 26, 189–222, https://doi.org/10.1023/A:1005734301837, 1997.

Holst, T., Arneth, A., Hayward, S., Ekberg, A., Mastepanov, M., Jackowicz-Korczynski, M., Friborg, T., Crill, P. M., and Bäckstrand, K.: BVOC ecosystem flux measurements at a high latitude wetland site, Atmospheric Chemistry and Physics, 10, 1617–1634, https://doi.org/10.5194/acp-10-1617-2010, 2010.

Holtslag, A., Svensson, G., Baas, P., Basu, S., Beare, B., Beljaars, A., Bosveld, F., Cuxart, J., Lindvall, J., Steeneveld, G., et al.: Stable atmospheric boundary layers and diurnal cycles: challenges for weather and climate models, Bulletin of the American Meteorological Society, 94, 1691–1706, https://doi.org/10.1175/BAMS-D-11-00187.1, 2013.

Hoppel, W., Fitzgerald, J., Frick, G., Caffrey, P., Pasternack, L., Hegg, D., Gao, S., Leaitch, R., Shantz, N., Cantrell, C., et al.: Particle formation and growth from ozonolysis of α-pinene, Journal of Geophysical Research: Atmospheres, 106, 27 603–27 618, https://doi.org/10.1029/2001JD900018, 2001.

Iinuma, Y., Böge, O., Miao, Y., Sierau, B., Gnauk, T., and Herrmann, H.: Laboratory studies on secondary organic aerosol formation from terpenes, Faraday Discussions, 130, 279–294, https://doi.org/10.1039/B502160J, 2005.

Jiang, J., Aksoyoglu, S., Ciarelli, G., Oikonomakis, E., El-Haddad, I., Canonaco, F., O'Dowd, C., Ovadnevaite, J., Minguillón, M. C., Baltensperger, U., et al.: Effects of two different biogenic emission models on modelled ozone and aerosol concentrations in Europe, Atmospheric Chemistry and Physics, 19, 3747–3768, https://doi.org/10.5194/acp-19-3747-2019, 2019.

https://doi.org/10.5194/egusphere-2026-352
Preprint. Discussion started: 13 February 2026

Jokinen, T., Berndt, T., Makkonen, R., Kerminen, V.-M., Junninen, H., Paasonen, P., Stratmann, F., Herrmann, H., Guenther, A. B., Worsnop, D. R., et al.: Production of extremely low volatile organic compounds from biogenic emissions: Measured yields and atmospheric implications, Proceedings of the National Academy of Sciences, 112, 7123–7128, https://doi.org/10.1073/pnas.1423977112, 2015.

Junninen, H., Lauri, A., Keronen, P., Aalto, P., Hiltunen, V., Hari, P., and Kulmala, M.: Smart-SMEAR: on-line data exploration and visualization tool for SMEAR stations, Boreal Environment Research, 14, 447, https://doi.org/10.60910/1frc-6day, 2009.

Kesselmeier, J. and Staudt, M.: Biogenic volatile organic compounds (VOC): an overview on emission, physiology and ecology, Journal of atmospheric chemistry, 33, 23–88, https://doi.org/10.1023/A:1006127516791, 1999.

Kleindienst, T. E., Edney, E. O., Lewandowski, M., Offenberg, J. H., and Jaoui, M.: Secondary Organic Carbon and Aerosol Yields from the Irradiations of Isoprene and α-Pinene in the Presence of NO x and SO2, Environmental science & technology, 40, 3807–3812, https://doi.org/10.1021/es052446r, 2006.

Kroll, J. H., Ng, N. L., Murphy, S. M., Flagan, R. C., and Seinfeld, J. H.: Secondary organic aerosol formation from isoprene photooxidation, Environmental science & technology, 40, 1869–1877, https://doi.org/10.1021/es0524301, 2006.

Kuenen, J., Dellaert, S., Visschedijk, A., Jalkanen, J.-P., Super, I., and Denier van der Gon, H.: CAMS-REG-v4: a state-of-the-art high-resolution European emission inventory for air quality modelling, Earth System Science Data, 14, 491–515, https://doi.org/10.5194/essd-14-491-2022, 2022.

Laffineur, Q., Aubinet, M., Schoon, N., Amelynck, C., Müller, J.-F., Dewulf, J., Van Langenhove, H., Steppe, K., Šimpraga, M., and Heinesch, B.: Isoprene and monoterpene emissions from a mixed temperate forest, Atmospheric Environment, 45, 3157–3168, https://doi.org/10.1016/j.atmosenv.2011.02.054, 2011.

Lane, T. E., Donahue, N. M., and Pandis, S. N.: Simulating secondary organic aerosol formation using the volatility basis-set approach in a chemical transport model, Atmospheric Environment, 42, 7439–7451, https://doi.org/10.1016/j.atmosenv.2008.06.026, 2008.

Laothawornkitkul, J., Taylor, J. E., Paul, N. D., and Hewitt, C. N.: Biogenic volatile organic compounds in the Earth system, New Phytologist, 183, 27–51, https://doi.org/10.1111/j.1469-8137.2009.02859.x, 2009.

Lee, J. Y., Xian, P., Selimovic, V., Booth, P.-P. M., Anderson, B. G., Liu, J., and Pratt, K. A.: Observation of Wildfire Smoke Particles That Accumulated Secondary Aerosol during Long-Range Transport, ACS Earth and Space Chemistry, 9, 2440–2454, https://doi.org/10.1021/acsearthspacechem.5c00172, 2025.

Lehtipalo, K., Yan, C., Dada, L., Bianchi, F., Xiao, M., Wagner, R., Stolzenburg, D., Ahonen, L. R., Amorim, A., Baccarini, A., et al.: Multicomponent new particle formation from sulfuric acid, ammonia, and biogenic vapors, Science advances, 4, eaau5363, https://doi.org/10.1126/sciadv.aau5363, 2018.

Lindfors, V. and Laurila, T.: Biogenic volatile organic compound (VOC) emissions from forests in Finland, Boreal environment research, 5, 95–113, https://doi.org/10.60910/ew2y-3ct1, 2000.

Lopez, B., Bhattacharyya, N., DeVivo, J., Wang, M., Caudillo-Plath, L., Surdu, M., Bianchi, F., Brasseur, Z., Buchholz, A., Chen, D., et al.: A diagonal volatility basis set to assess the condensation of organic vapors onto particles, Environmental Science: Atmospheres, 5, 1035–1061, https://doi.org/10.1039/D5EA00062A, 2025.

Mäki, M., Aalto, J., Hellén, H., Pihlatie, M., and Bäck, J.: Interannual and seasonal dynamics of volatile organic compound fluxes from the boreal forest floor, Frontiers in plant science, 10, 191, https://doi.org/10.3389/fpls.2019.00191, 2019.

Mazzeo, A., Burrow, M., Quinn, A., Marais, E. A., Singh, A., Ng'ang'a, D., Gatari, M. J., and Pope, F. D.: Evaluation of the WRF and CHIMERE models for the simulation of PM2. 5 in large East African urban conurbations, Atmospheric Chemistry and Physics, 22, 10 677–10 701, https://doi.org/10.5194/acp-22-10677-2022, 2022.

https://doi.org/10.5194/egusphere-2026-352
Preprint. Discussion started: 13 February 2026

McFiggans, G., Mentel, T. F., Wildt, J., Pullinen, I., Kang, S., Kleist, E., Schmitt, S., Springer, M., Tillmann, R., Wu, C., et al.: Secondary organic aerosol reduced by mixture of atmospheric vapours, Nature, 565, 587–593, https://doi.org/10.1038/s41586-018-0871-y, 2019.

Menut, L., Cholakian, A., Pennel, R., Siour, G., Mailler, S., Valari, M., Lugon, L., and Meurdesoif, Y.: The CHIMERE chemistry-transport model v2023r1, Geoscientific Model Development Discussions, 2024, 1–44, https://doi.org/10.5194/gmd-17-5431-2024, 2024.

Messina, P., Lathière, J., Sindelarova, K., Vuichard, N., Granier, C., Ghattas, J., Cozic, A., and Hauglustaine, D. A.: Global biogenic volatile organic compound emissions in the ORCHIDEE and MEGAN models and sensitivity to key parameters, Atmospheric Chemistry and Physics, 16, 14 169–14 202, https://doi.org/10.5194/acp-16-14169-2016, 2016.

Murphy, B. N. and Pandis, S. N.: Simulating the formation of semivolatile primary and secondary organic aerosol in a regional chemical transport model, Environmental science & technology, 43, 4722–4728, https://doi.org/10.1021/es803168a, 2009.

Nenes, A., Pandis, S. N., and Pilinis, C.: ISORROPIA: A new thermodynamic equilibrium model for multiphase multicomponent inorganic aerosols, Aquatic geochemistry, 4, 123–152, https://doi.org/10.1023/A:1009604003981, 1998.

Ng, N. L., Kroll, J. H., Keywood, M. D., Bahreini, R., Varutbangkul, V., Flagan, R. C., Seinfeld, J. H., Lee, A., and Goldstein, A. H.: Contribution of first-versus second-generation products to secondary organic aerosols formed in the oxidation of biogenic hydrocarbons, Environmental science & technology, 40, 2283–2297, https://doi.org/10.1021/es052269u, 2006.

Niinemets, Ü., Kuhn, U., Harley, P. C., Staudt, M., Arneth, A., Cescatti, A., Ciccioli, P., Copolovici, L., Geron, C., Guenther, A., et al.: Estimations of isoprenoid emission capacity from enclosure studies: measurements, data processing, quality and standardized measurement protocols, Biogeosciences, 8, 2209–2246, https://doi.org/10.5194/bg-8-2209-2011, 2011.

Olonimoyo, E. A., Ahn, M. C., Rastogi, D., Li, Y., Duncan, C. M., and Asa-Awuku, A.: Chemical signatures of water-soluble organic carbon (WSOC) fraction of long-range transported wildfire PM 2.5 from Canada to the United States Mid-Atlantic region, Environmental Science: Atmospheres, https://doi.org/10.1039/D5EA00119F, 2026.

Opacka, B., Müller, J.-F., Stavrakou, T., Bauwens, M., Sindelarova, K., Markova, J., and Guenther, A. B.: Global and regional impacts of land cover changes on isoprene emissions derived from spaceborne data and the MEGAN model, Atmospheric Chemistry and Physics, 21, 8413–8436, https://doi.org/10.5194/acp-21-8413-2021, 2021.

Ortiz-Amezcua, P., Guerrero-Rascado, J. L., Granados-Muñoz, M. J., Benavent-Oltra, J. A., Böckmann, C., Samaras, S., Stachlewska, I. S., Janicka, Ł., Baars, H., Bohlmann, S., et al.: Microphysical characterization of long-range transported biomass burning particles from North America at three EARLINET stations, Atmospheric Chemistry and Physics, 17, 5931–5946, https://doi.org/10.5194/acp-17-5931-2017, 2017.

Paasonen, P., Asmi, A., Petäjä, T., Kajos, M. K., Äijälä, M., Junninen, H., Holst, T., Abbatt, J. P., Arneth, A., Birmili, W., et al.: Warming-induced increase in aerosol number concentration likely to moderate climate change, Nature Geoscience, 6, 438–442, https://doi.org/10.1038/ngeo1800, 2013.

Pathak, R. K., Stanier, C. O., Donahue, N. M., and Pandis, S. N.: Ozonolysis of α-pinene at atmospherically relevant concentrations: Temperature dependence of aerosol mass fractions (yields), Journal of Geophysical Research: Atmospheres, 112, https://doi.org/10.1029/2006JD007436, 2007.

Peñuelas, J. and Staudt, M.: BVOCs and global change, Trends in plant science, 15, 133–144, https://doi.org/10.1016/j.tplants.2009.12.005, 2010.

Petäjä, T., Tabakova, K., Manninen, A., Ezhova, E., O'Connor, E., Moisseev, D., Sinclair, V., Backman, J., Levula, J., Luoma, K., et al.: Influence of biogenic emissions from boreal forests on aerosol–cloud interactions, Nature Geoscience, 15, 42–47, https://doi.org/10.1038/s41561-021-00876-0, 2022.

https://doi.org/10.5194/egusphere-2026-352
Preprint. Discussion started: 13 February 2026

Prentice, I. C., Cramer, W., Harrison, S. P., Leemans, R., Monserud, R. A., and Solomon, A. M.: Special paper: a global biome model based on plant physiology and dominance, soil properties and climate, Journal of biogeography, pp. 117–134, https://doi.org/10.2307/2845499, 1992.

Presto, A. A., Huff Hartz, K. E., and Donahue, N. M.: Secondary organic aerosol production from terpene ozonolysis. 2. Effect of NO x concentration, Environmental Science & Technology, 39, 7046–7054, https://doi.org/10.1021/es050400s, 2005.

Rantala, P., Taipale, R., Aalto, J., Kajos, M. K., Patokoski, J., Ruuskanen, T. M., and Rinne, J.: Continuous flux measurements of VOCs using PTR-MS-reliability and feasibility of disjunct-eddy-covariance, surface-layer-gradient, and surface-layer-profile methods, Boreal Environment Research, 19, 87–107, https://doi.org/10.5555/20153028006, 2014.

Riccobono, F., Schobesberger, S., Scott, C. E., Dommen, J., Ortega, I. K., Rondo, L., Almeida, J., Amorim, A., Bianchi, F., Breitenlechner, M., et al.: Oxidation products of biogenic emissions contribute to nucleation of atmospheric particles, Science, 344, 717–721, https://doi.org/10.1126/science.1243527, 2014.

Riuttanen, L., Hulkkonen, M., Dal Maso, M., Junninen, H., and Kulmala, M.: Trajectory analysis of atmospheric transport of fine particles, SO 2, NO x and O 3 to the SMEAR II station in Finland in 1996–2008, Atmospheric Chemistry and Physics, 13, 2153–2164, https://doi.org/10.5194/acp-13-2153-2013, 2013.

Seinfeld, J. H. and Pandis, S. N.: Atmospheric chemistry and physics: from air pollution to climate change, John Wiley & Sons, 2016.

Silva, S. J., Heald, C. L., and Guenther, A. B.: Development of a reduced-complexity plant canopy physics surrogate model for use in chemical transport models: A case study with GEOS-Chem v12. 3.0, Geoscientific Model Development, 13, 2569–2585, https://doi.org/10.5194/gmd-13-2569-2020, 2020.

Simpson, D., Benedictow, A., Berge, H., Bergström, R., Emberson, L. D., Fagerli, H., Flechard, C. R., Hayman, G. D., Gauss, M., Jonson, J. E., et al.: The EMEP MSC-W chemical transport model–technical description, Atmospheric Chemistry and Physics, 12, 7825–7865, https://doi.org/10.5194/acp-12-7825-2012, 2012.

Sindelarova, K., Granier, C., Bouarar, I., Guenther, A., Tilmes, S., Stavrakou, T., Müller, J.-F., Kuhn, U., Stefani, P., and Knorr, W.: Global data set of biogenic VOC emissions calculated by the MEGAN model over the last 30 years, Atmospheric Chemistry and Physics, 14, 9317–9341, https://doi.org/10.5194/acp-14-9317-2014, 2014.

Sindelarova, K., Markova, J., Simpson, D., Huszar, P., Karlicky, J., Darras, S., and Granier, C.: High-resolution biogenic global emission inventory for the time period 2000–2019 for air quality modelling, Earth System Science Data, 14, 251–270, https://doi.org/10.5194/essd-14-251-2022, 2022.

Skamarock, W. C., Klemp, J. B., Dudhia, J., Gill, D. O., Liu, Z., Berner, J., Wang, W., Powers, J. G., Duda, M. G., Barker, D. M., et al.: A description of the advanced research WRF version 4, NCAR tech. note ncar/tn-556+ str, 145, 2019.

Stolzenburg, D., Cai, R., Blichner, S. M., Kontkanen, J., Zhou, P., Makkonen, R., Kerminen, V.-M., Kulmala, M., Riipinen, I., and Kangasluoma, J.: Atmospheric nanoparticle growth, Reviews of Modern Physics, 95, 045 002, https://doi.org/10.1103/RevModPhys.95.045002, 2023.

Takekawa, H., Minoura, H., and Yamazaki, S.: Temperature dependence of secondary organic aerosol formation by photo-oxidation of hydrocarbons, Atmospheric Environment, 37, 3413–3424, https://doi.org/10.1016/S1352-2310(03)00359-5, 2003.

Tarvainen, V., Hakola, H., Hellén, H., Bäck, J., Hari, P., and Kulmala, M.: Temperature and light dependence of the VOC emissions of Scots pine, Atmospheric Chemistry and Physics, 5, 989–998, https://doi.org/10.5194/acp-5-989-2005, 2005.

https://doi.org/10.5194/egusphere-2026-352
Preprint. Discussion started: 13 February 2026

Theobald, M. R., Vivanco, M. G., Aas, W., Andersson, C., Ciarelli, G., Couvidat, F., Cuvelier, K., Manders, A., Mircea, M., Pay, M.-T., et al.: An evaluation of European nitrogen and sulfur wet deposition and their trends estimated by six chemistry transport models for the period 1990–2010, Atmospheric Chemistry and Physics, 19, 379–405, https://doi.org/10.5194/acp-19-379-2019, 2019.

Tunved, P., Hansson, H.-C., Kerminen, V.-M., Strom, J., Maso, M. D., Lihavainen, H., Viisanen, Y., Aalto, P. P., Komppula, M., and Kulmala, M.: High natural aerosol loading over boreal forests, Science, 312, 261–263, https://doi.org/10.1126/science.1123052, 2006.

Vettikkat, L., Miettinen, P., Buchholz, A., Rantala, P., Yu, H., Schallhart, S., Petäjä, T., Seco, R., Männistö, E., Kulmala, M., et al.: High emission rates and strong temperature response make boreal wetlands a large source of isoprene and terpenes, Atmospheric Chemistry and Physics, 23, 2683–2698, https://doi.org/10.5194/acp-23-2683-2023, 2023.

Vitali, B., Bettineschi, M., Cholakian, A., Zardi, D., Bianchi, F., Sinclair, V. A., Mikkola, J., Cristofanelli, P., Marinoni, A., Mazzini, M., et al.: Analysis of chemical and transport processes of biogenic aerosols over the northern Apennines: insights from the WRF-CHIMERE model, Environmental Science: Atmospheres, 4, 967–987, https://doi.org/10.1039/D4EA00040D, 2024.

Wang, H., Liu, X., Wu, C., and Lin, G.: Regional to global distributions, trends, and drivers of biogenic volatile organic compound emission from 2001 to 2020, Atmospheric Chemistry and Physics, 24, 3309–3328, https://doi.org/10.5194/acp-24-3309-2024, 2024a.

Wang, L., Lun, X., Wang, Q., and Wu, J.: Biogenic volatile organic compounds emissions, atmospheric chemistry, and environmental implications: a review, Environmental Chemistry Letters, 22, 3033–3058, https://doi.org/10.1007/s10311-024-01785-5, 2024b.

Weng, H., Lin, J., Martin, R., Millet, D. B., Jaeglé, L., Ridley, D., Keller, C., Li, C., Du, M., and Meng, J.: Global high-resolution emissions of soil NOx, sea salt aerosols, and biogenic volatile organic compounds, Scientific Data, 7, 148, https://doi.org/10.1038/s41597-020-0488-5, 2020.

Yli-Juuti, T., Mielonen, T., Heikkinen, L., Arola, A., Ehn, M., Isokääntä, S., Keskinen, H.-M., Kulmala, M., Laakso, A., Lipponen, A., et al.: Significance of the organic aerosol driven climate feedback in the boreal area, Nature Communications, 12, 5637, https://doi.org/10.1038/s41467-021-25850-7, 2021.

Zhang, J., Huff Hartz, K. E., Pandis, S. N., and Donahue, N. M.: Secondary organic aerosol formation from limonene ozonolysis: Homogeneous and heterogeneous influences as a function of NO x, The Journal of Physical Chemistry A, 110, 11 053–11 063, https://doi.org/10.1021/jp062836f, 2006.

Zhao, T., Mao, J., Ayazpour, Z., González Abad, G., Nowlan, C. R., and Zheng, Y.: Interannual variability of summertime formaldehyde (HCHO) vertical column density and its main drivers at northern high latitudes, Atmospheric Chemistry and Physics, 24, 6105–6121, https://doi.org/10.5194/acp-24-6105-2024, 2024.